Silk fibres grafted with 2-hydroxyethyl methacrylate (HEMA) and 4-hydroxybutyl acrylate (HBA) for biomedical applications

Abstract

Silk fibroin may be chemically modified by grafting, with the purpose of improving its properties according to the desired function. In this study, silk fabrics from *Bombyx mori* silk fibres were grafted with 2-hydroxyethyl methacrylate (HEMA), as well as a binary mixture of HEMA and 4-hydroxybutyl acrylate (HBA). The samples were then electrospun from trifluoroacetic acid and treated with aqueous methanol. The % weight gains ascribable to HEMA and HBA were successfully determined through Raman spectroscopy. PolyHEMA made the fibres more hydrophilic and hindered crystallization into β-sheet only upon electrospinning and treatment with aqueous methanol; the presence of the HBA component in the grafting mixture did not further decrease the ability of silk fibroin to rearrange into β-sheet, due to its low contents (below 5%) under the used experimental conditions. Fibrillation partially occurred in the grafted fabrics; the electrospun samples maintained their nanostructured morphology. The surface of the substrates under investigation was compatible with cell attachment and growth, which were higher for the nanofibres. Cell adhesion and proliferation may be modulated by varying the surface chemistry and topography of the fabrics; grafting improved the surface properties of silk fibroin for enhanced functional performance in view of biomedical applications.

Keywords: electrospinning; vibrational spectroscopy; fibroblasts culture.

SILK FIBRES GRAFTED WITH 2-HYDROXYETHYL METHACRYLATE (HEMA) AND 4-HYDROXYBUTYL ACRYLATE (HBA) FOR BIOMEDICAL APPLICATIONS

Paola Taddei,[1*] Michele Di Foggia,[1] Simona Martinotti,[2] Elia Ranzato,[3] Irene Carmagnola,[4] Valeria Chiono,[4] Masuhiro Tsukada[5]

[1] Department of Biomedical and Neuromotor Sciences, University of Bologna, Via Belmeloro 8/2, 40126 Bologna, Italy.

[2] Department of Sciences and Technological Innovation, University of Eastern Piedmont, Viale Teresa Michel 11, 15121 Alessandria, Italy.

[3] Department of Sciences and Technological Innovation, University of Eastern Piedmont, Piazza Sant'Eusebio 5, 13100 Vercelli, Italy.

[4] Department of Mechanical and Aerospace Engineering, Politecnico di Torino, Corso Duca degli Abruzzi 24, 10129 Turin, Italy.

[5] Division of Applied Biology, Faculty of Textile Science and Technology, Shinshu University, Ueda, Nagano, Japan.

Corresponding author:
Prof. Paola Taddei
Dipartimento di Scienze Biomediche e Neuromotorie
Via Belmeloro 8/2
40126 BOLOGNA, ITALY
phone and fax: +39 051 2094280
e-mail: paola.taddei@unibo.it

1. INTRODUCTION

Silks are fibrous proteins characterized by outstanding tensile properties and high biocompatibility, which make them useful in biomedical applications [1]. Silk fibres can be obtained from a wide variety of silkworms, such as domesticated *Bombyx mori*, and spiders [2]. The specific and remarkable properties of *B. mori* silk derive from its structure, which consists of a core containing at least two main fibroin proteins (light and heavy chains, of 25 and 325 kDa, respectively), coated by sericin, a water soluble glue-like protein. Silk fibroin as such or properly modified by chemical and enzymatic methods has gained increasing attention in biomedical applications, due to its environmental stability, outstanding mechanical properties, controlled proteolytic biodegradation, and morphologic flexibility [1-10].

In this context, electrospinning has proved a very useful technique to extend silk fibroin applications, since it allows to obtain fibres characterized by a porous structure and diameters ranging between nanoscale and microscale orders [8,9]; the electrospun nanofibres have been used as substrates for drug delivery systems, wound dressing and tissue engineering [1,2,6,7,10].

Among the chemical methods exploited to modify the silk fibre surface, grafting proved to be a superior way to attain long-lasting modifications due to covalent bond formation. With the purpose of improving the textile properties of silk, the graft copolymerization of vinyl monomers onto silk has been introduced in Japan in the early 1960s and has been widely applied in the textile industry [11]. The graft copolymerization utilizes grafting agents that enable to modify the silk properties depending on the grafting extent, the molecular weight of the grafted polymer as well as its functional groups [12-14]. In particular, 2-hydroxyethyl methacrylate (HEMA) and 4-hydroxybutyl acrylate (HBA) have been used to modify silk due to their peculiarity of increasing comfort and easy-care properties, while preserving handle and drape [15,16]. On the other hand, polyHEMA has been used since the early 1960s in

several biomedical applications (i.e. as component of dental adhesives, in soft contact lenses, vascular grafts, soft tissue substitutes and drug delivery systems) [17-20], thanks to its biocompatibility, high permeability to small metabolites, high hydrophilicity and resistance to adhesion of blood proteins and cells. Also polyHBA has been proposed as hydrogel [21]. HBA has been used as copolymer building block for biomedical applications [22], such as tissue engineering [23] and drug delivery systems [24].

In the light of these findings, we tested the possibility of using HEMA- and HBA-grafted silk fibroin (designed for textile purposes) also for biomedical applications, as scaffold for soft tissue engineering. HEMA and HBA have a hydrophilic OH group at the end of their side chain, which is slightly longer in the latter. The balance of hydrophilicity and hydrophobicity of the surface of silk fibroin may be modified by varying the HEMA and HBA contents, which is useful in the design of biomaterials for tissue engineering. In this context, Dhyani and Singh [25] have reported that the graft polymerization of polyHEMA on *B. mori* silk fibroin films is a good strategy able to improve cell proliferation and adhesion in view of tissue engineering applications.

In a previous study [26], *B. mori* silk fabrics were successfully modified by grafting with HEMA and a binary mixture of HEMA and HBA; the grafted silk and pure control silk fabrics were solubilized in trifluoroacetic acid (TFA), electrospun and subsequently immersed in aqueous methanol, to induce the rearrangement of the as-electrospun nanofibres (mainly characterized by unordered/Silk I conformations) [27] towards an insoluble β-sheet structure [28]. Preliminary vibrational analyses of the obtained devices allowed to clarify the role played by the grafted polymer on the silk conformation [26].

In the present study, a more complete vibrational characterization was carried out and the samples were further assessed by SEM imaging, in view of their possible applications as biomedical devices. Contact angle measurements were carried out to evaluate the possible surface hydrophilicity changes induced by grafting; this information was correlated with

vibrational data. NIH 3T3 fibroblast cell line was employed to study the biological response of the substrates, with the aim to demonstrate their suitability for possible biomedical applications. To the best of our knowledge, our work represents the first study on the biocompatibility of silk fabrics and nanofibres grafted with HEMA and HEMA/HBA.

2. MATERIALS AND METHODS

2.1 Materials and grafting

B. mori silk fabrics were dewaxed with a binary methanol/benzene (50/50 v/v) mixture at 30°C for 3 days. HEMA and HBA were purchased from Wako Pure Chemical Industries Ltd., Tokyo and were used without further purification.

The silk fabric grafted with HEMA (indicated hereafter as HEMA35-grafted sample) was prepared as previously reported [26], using a grafting system containing 35% owf (over weight fibre) HEMA and 2.5% owf ammonium persulfate (APS) as initiator, at pH 3 and 80°C. At the end of the reaction, the HEMA-grafted silk fabric was extracted with acetone to remove unreacted monomer, washed with boiling water, dried and weighed.

To obtain the silk fabrics grafted with HEMA and HBA, the reaction was performed under the same conditions, using binary mixtures containing 25% owf HEMA and 10% owf HBA (first experiment, HEMA25_HBA10-grafted sample) and 30% owf HEMA and 5% owf HBA (second experiment, HEMA30_HBA5-grafted sample). Silk fabrics grafted with HBA were prepared for comparison [26]. The grafting system contained different amounts of HBA (i.e. 20%, 35%, 45%, 54%, 100% owf).

The percentage weight gain (w.g.) of the prepared samples was determined according to the following equation:

$$\%\ \text{weight gain} = \frac{W_t - W_0}{W_0} \times 100 \qquad (1)$$

where W_0 was the initial weight of the dry fabric, and W_t was the weight of the fabric after grafting, washing and drying.

2.2 Electrospinning and aqueous methanol treatment

The control silk fabric, the HEMA35-grafted, HEMA25_HBA10-grafted and HEMA30_HBA5-grafted fabrics were electrospun from trifluoroacetic acid (TFA, Wako Pure Chemical Industries Ltd. Tokyo, Japan, used without further purification) at 8 wt% concentration, under the experimental conditions previously reported [26].

All the nanofibres were immersed in 50% v/v aqueous methanol solution for 10 minutes, rinsed with water and allowed to dry at room temperature for 12 h.

2.3 Raman and IR vibrational spectroscopy

Raman spectra were recorded on a Bruker MultiRam FT-Raman spectrometer equipped with a cooled Ge-diode detector. The excitation source was a Nd^{3+}-YAG laser (1064 nm) in the backscattering (180°) configuration. The focused laser beam diameter was about 100 μm and the spectral resolution 4 cm^{-1}. Laser power at the sample was about 40 mW.

The Raman Amide I region was analyzed by a curve-fitting procedure to evaluate the content of secondary structures. A 2-points linear baseline correction in the 1750–1580 cm^{-1} spectral range was made prior to this procedure. The curve-fitting analysis was performed using the OPUS version 6.5 program (Bruker Optik GmbH), which uses the Levenberg–Marquardt algorithm.

Band fitting was performed according to Lefèvre *et al.* [29] with five amide I components located at about 1640, 1656, 1667 cm^{-1} (assigned to unordered conformations, 3_1 helices and β-sheet, respectively [29]), 1680 and 1695 cm^{-1} (assigned to β-turns [29]), and two bands at about 1597 and 1615 cm^{-1} associated with side-chain vibrations of aromatic residues. In addition, bands ascribable to the grafted polymers or protonated glutamate and aspartate residues were used when necessary.

The Raman component profiles were described as a linear combination of Lorentzian and Gaussian functions; the band widths and the percentages of the Lorentzian character were fixed according to Lefèvre *et al.* [29]. The area of each component divided by the sum of the

area of all amide I components was used for the determination of each secondary structure content.

IR spectra were recorded on a Nicolet 5700 FTIR spectrometer, equipped with a Smart Orbit diamond ATR accessory and a DTGS detector; the spectral resolution was 4 cm^{-1} with 64 scans for each spectrum. The ATR technique allows to investigate the surface skin of the specimens (under the used experimental conditions, the investigated sample thickness was about 2 μm). Both IR and Raman spectra were recorded in triplicate.

2.4 Morphological analysis: Scanning Electron Microscopy

The morphology of silk fabrics and silk nanofibres before and after methanol treatment was evaluated through Scanning Electron Microscopy (SEM). Samples were coated with a thin gold layer using Agar Auto Sputter Coater. Then the samples were analysed through SEM LEO – 1430 (Zeiss) equipment at different magnifications (500×, 1000×, 2000× and 5000×). The average fiber diameter size of the samples was calculated using ImageJ software. Results were reported as average value ± standard deviation (SD).

2.5 Contact angle measurements

Static contact angles were measured at room temperature using a CAM 200 Instrument (KSV NIMA, Biolin Scientific, Finland) equipped with an Attention Theta software (Biolin Scientific, Finland) for data acquisition. Three Milli-Q water droplets (volume 5 μL) were deposited on each sample and data were collected thereafter for 10 s with a time frame of 10 ms. The data were expressed as mean value ± SD. Statistical analysis was carried out using single-factor analysis of variance (ANOVA). Values of $P < 0.05$ were considered statistically significant.

2.6 Cell culture and vitality assessment

Murine fibroblasts NIH 3T3 cells were obtained from American Type Culture Collection (Cat. no. ATCC CRL-1658, http://www.lgcstandards-atcc.org). Cells were cultured at 37°C,

in a humidified atmosphere with 5% CO_2, in DMEM with 10% fetal calf serum (FBS) and 1% antibiotic mixture (Sigma-Aldrich, Milan, Italy).

The fabrics and the methanol-treated nanofibrous scaffolds were sterilized by UV irradiation for 1 hour. Cells were incubated at standard culture conditions on all the samples for 1 and 3 days.

The number of viable cells was estimated with calcein-AM assay. The Calcein-AM kit provides a simple, rapid, and accurate method to measure cell viability and/or cytotoxicity. Calcein-AM is a non-fluorescent, hydrophobic compound that easily permeates intact, live cells. The hydrolysis of Calcein-AM by intracellular esterases produces calcein, a hydrophilic, strongly fluorescent compound that is well-retained in the cell cytoplasm.

For calcein-AM assays, cells were settled overnight in 96-well plates (8,000 cells/well) and then incubated with the samples under study (i.e. fabrics and nanofibres). After incubation, cells were washed with PBS, and then incubated for 30 min at 37°C with 2.5 μM calcein-acetoxymethylester (calcein-AM) in PBS. Plates were read in an Infinite 200 Pro plate reader (Tecan, Wien, Austria). The fluorescence was read using a 485 nm excitation filter and a 535 nm emission filter [30]. Data were analyzed by ANOVA and the post hoc Tukey's test, using the Instat software package (GraphPad Software, Inc, San Diego, CA).

3. RESULTS

3.1 Spectroscopic characterization: fabrics

Fig. 1 (A) and Fig. S1, Supplementary Material (SM), show the Raman and IR spectra of HEMA35-grafted, HEMA30_HBA5-grafted and HEMA25_HBA10-grafted silk fabrics (w.g. 26%, 24% and 20%, respectively). The spectra of control silk fabric and polyHEMA have been previously reported [26] and are here shown for comparison.

Upon grafting, both Raman and IR spectra showed spectral features ascribable to polyHEMA [26, 31-33] (indicated with asterisks in Fig. 1 (A) and Fig. S1, SM).

To investigate the effective incorporation of the HBA component into the samples grafted with binary mixtures of HEMA and HBA, the marker bands due to the HBA-grafting were identified by inspecting the Raman and IR spectra of the HBA-grafted samples (with weight gains ranging between 9.7% and 57%). As can be seen from Fig. S2 and S3, SM, bands assignable to the HBA component were observed with increasing intensity at increasing weight gain at 1728, 1451, 1300, 1266, 1043, 829, 810 cm^{-1} (Raman) and 1729, 1700, 1434, 1398, 1260, 1160, 1061, 1038, 996 and 940 cm^{-1} (IR).

The Raman and IR spectra of HEMA30_HBA5-grafted and HEMA25_HBA10-grafted fabrics (Fig. 1 and Fig. S1, SM) showed that also the HBA component was incorporated into the fabric, as shown by the appearance of its above marker bands at 1300 and 1043 cm^{-1} (Raman) and 1160 and 1040 cm^{-1} (IR).

The Raman I_{602}/I_{644} and I_{1300}/I_{644} intensity ratios were identified as useful spectral markers to obtain quantitative information on the HEMA and HBA incorporation, respectively. The band at 602 cm^{-1} was chosen since it was the strongest polyHEMA band falling in a spectral range free from silk fibroin bands (see Fig. 1 (A)). An analogous reason motivates the choice of the band at 1300 cm^{-1} for the quantification of the HBA incorporation: this is the most intense spectral feature falling in a region relatively free from silk fibroin bands (see Fig. S2, SM). Both the I_{602}/I_{644} and I_{1300}/I_{644} ratios were found to well correlate with the sample weight gain in samples grafted with only HEMA or HBA (R^2 values of 0.9735 and 0.9886, respectively, Fig. S4, SM). The plot reported in Fig. S4 (A), SM, shows the trend of the I_{602}/I_{644} intensity ratio as a function of % weight gain as calculated from the Raman spectrum of the HEMA35-grafted fabric (Fig. 1 (A)) as well as from data reported in the literature on other HEMA-grafted samples (with weight gains of 18.1% and 47.7%) [12]. Fig. S4 (B), SM, shows the trend of the I_{1300}/I_{644} intensity ratio (calculated from the spectra reported in Fig. S2, SM) as a function of the % weight gain. The good R^2 values obtained for the lines reported in Fig. S4 (A) and (B), SM, allowed their use for the quantitative determination of HEMA and HBA

incorporation into the HEMA30_HBA5-grafted and HEMA25_HBA10-grafted fabrics. The I_{602}/I_{644} and I_{1300}/I_{644} intensity ratios were calculated from their Raman spectra (Fig. 1 (A)) and these values were used to calculate the weight gains corresponding to the single HEMA and HBA components (Fig. 1 (B)), by interpolation from the lines reported in Fig. S4 (A) and (B), SM.

The possible occurrence of changes in silk fibroin conformation upon grafting has been investigated. The spectra reported in Fig. 1 (A) and Fig. S1, SM, showed that all the grafted samples had a prevailing β-sheet conformation, as shown by the Raman bands at about 1664 cm^{-1} (Amide I), 1229 cm^{-1} (Amide III), 1162, 1084, 975 and 882 cm^{-1} (CC stretching, CC skeletal stretching, CH_3 rocking and CH_2 rocking of a β-sheet conformations, respectively [34-36]), and by the IR bands at 1698-1618 cm^{-1} (Amide I), 1514 cm^{-1} (Amide II), 1264-1226 cm^{-1} (Amide III) [37-39], 997 and 974 cm^{-1} (Ala-Gly sequences in β-sheet conformation [37]), although in some of these spectral ranges the contribution of polyHEMA was revealed. The full-width at half maximum of the Raman Amide I band (FWHM) was nearly the same in the spectra of all the fabrics, as shown in Fig. 2 (A).

To gain information on the secondary structure distribution, the Raman Amide I of the samples under study was fitted into their components (see Fig. S5, SM, for some examples), as detailed in the Experimental section. Amide I band fitting data (Fig. 2(B)) showed that the HEMA35, HEMA30_HBA5 and HEMA25_HBA10-grafted fabrics had secondary structure contents not significantly different from those of the silk control sample and confirmed that upon grafting the prevailing conformation remained β-sheet. It may be noted that the secondary structure distribution obtained for the silk control fabric was in good agreement with the data reported by Lefèvre *et al.* [29].

An analogous conformational study was carried out on the spectra of the HBA-grafted samples reported in Fig. S2 and S3, SM. The shift of the Raman Amide I band towards higher wavenumber values, the weakening of the above mentioned marker bands of β-sheet

conformation (Fig. S2, SM), and the appearance of an IR Amide II component at 1540 cm^{-1} (Fig. S3, SM) revealed that silk fibroin underwent conformational rearrangements upon grafting with HBA. The Raman Amide I fitting data (Fig. S6, SM) showed that at a weight gain of 9.7% the silk fibroin underwent significant changes in β-sheet and β-turns conformations, which persisted at nearly the same extents at higher weight gains.

To separately investigate the relative effects of the HEMA and HBA grafting on silk fibroin conformational rearrangements, the Raman spectra of HEMA-grafted and HBA-grafted fabrics with similar weight gains (i.e. 26% and 25%, respectively) were compared; as shown in Fig. 3 (A), the HBA-grafted sample showed a broader Amide I band, shifted to higher wavenumber values compared to the HEMA-grafted sample. The band fitting data (Fig. 3 (B)) showed that the former had a lower content of β-sheet and higher amounts of β-turns.

3.2 Spectroscopic characterization: nanofibres after immersion in aqueous methanol

Fig. 4 shows the Raman and IR spectra of electrospun HEMA35-grafted, HEMA30_HBA5-grafted and HEMA25_HBA10-grafted nanofibres after immersion in aqueous methanol. The spectra of control silk nanofibres treated under the same conditions have been previously reported [26] and are here shown for comparison.

The spectra of all the samples showed the above mentioned Raman and IR marker bands of β-sheet conformation. However, some spectral features revealed that the nanofibres were conformationally more heterogeneous than the corresponding fabrics from which they were obtained. In fact, as shown in Fig. 2 (A), the full-width at half maximum (FWHM) of the Raman Amide I band increased in all the samples upon electrospinning and subsequent immersion in aqueous methanol. The band fitting data reported in Fig. 2 (B) showed that upon these treatments, the samples underwent significant increases in the contents of β-turns and unordered conformations, at the expenses of β-sheet, whose amount decreased.

The higher structural heterogeneity of the nanofibres with respect to the corresponding fabrics was confirmed by the IR spectra (Fig. 4 (B)), which showed for all the samples bands

assignable to Silk I [40] at about 1416, 1370, 1335 and 1019 cm^{-1}, together with those of β-sheet and unordered conformations [41].

It is interesting to note that the band at about 1725 cm^{-1}, which appeared in both IR and Raman spectra (Fig. 4) of the grafted nanofibres, appeared also in control silk sample [26]; therefore, besides to the grafted polymer, it is also assignable to the C=O stretching mode of the COOH group of aspartic and glutamic acids. These residues, according to previous studies [26,42], undergo protonation upon dissolution in TFA, since the pK_a value of this solvent is significantly lower than the pK_a values of the carboxylic groups of the amino acids (pK_a = 0.2 *versus* 3.7 and 4.3 for aspartic and glutamic acids, respectively).

3.3 Morphological analysis

Fig. 5 reports the SEM images of the fabrics under study as well as of the nanofibres before and after aqueous methanol treatment. The images of the control silk fabric show a smooth surface, whereas the grafted silk fabrics show the occurrence of fibrillation, due to the grafting treatment. The average fibre diameter in silk fabrics was not affected by the grafting treatment, as shown in Fig. S7, SM, and was about 12 μm in all the samples.

The membranes obtained by electrospinning of pure and grafted silk samples were free of defects and homogenous in morphology. The average diameter of the as-electrospun fibres was about 300 nm (Fig. S7, SM). After aqueous methanol treatment, all the analyzed nanofibrous membranes maintained their fibrous structure and the average fibre diameters slightly increased up to ~500 nm (Fig. S7, SM). Moreover, the electrospun scaffolds, before and after aqueous methanol treatment, showed a quite homogeneous diameter distribution, which was comprised between 100 and 500 nm (Fig. S7, SM).

The analysis of the pore dimension distribution (Fig. S8, SM) showed that the pore size distribution did not change after the aqueous methanol treatment.

3.4 Contact angle measurements

Contact angle values, measured through static contact angle equipment, are shown in Fig. 6

(A).

In general, fabric samples showed lower wettability if compared to the electrospun samples. HEMA grafting significantly affected the surface contact angle; going from control silk to the HEMA35-grafted samples, its value decreased from 128° ± 2 to 112° ± 4 in the fabrics, and from 104° ± 3 to 81° ± 3 in the nanofibres. Upon adding HBA in the grafting mixture (i.e. in the HEMA30_HBA5-grafted and HEMA25_HBA10-grafted samples), the contact angle was found to slightly increase with respect to the HEMA35-grafted samples.

As shown in Fig. 6 (B), the contact angle value was found to well correlate with the % HEMA weight gain (determined by weight measurements for HEMA35-grafted samples and by Raman spectroscopy for HEMA30_HBA5-grafted and HEMA25_HBA10-grafted samples, data reported in Fig. 1 (B)).

3.5 Cell viability of fibroblasts

Fig. 7 shows the cellular viability determined by calcein-AM assay for NIH 3T3 fibroblasts cultured on to different materials (i.e. silk, HEMA35-grafted, HEMA30_HBA5-grafted and HEMA25_HBA10-grafted silk fabrics and methanol-treated nanofibres) for 1 and 3 days culture time.

As shown in Fig. 7 (A), after 1 day, most fabrics allowed a cell growth rate similar to that of the cells in the culture well; the HEMA25_HBA10-grafted silk fabric was the only material that induced a significant improvement in cell proliferation. After 3 days, the growth of cells on the fabrics markedly decreased on HEMA35 and HEMA30_HBA5-grafted silk fabrics while, in the case of HEMA25_HBA10-grafted silk fabric, the fibroblasts partly lost their potential growth observed at 1 day, although they still showed a higher proliferation than on the control silk fabric.

The same experiment was carried out on the electrospun nanofibres treated with aqueous methanol; the data reported in Fig. 7 (B) show that after 3 days, the nanofibrous membranes behaved better than the corresponding fabrics at the same culture time.

4. DISCUSSION

The vibrational spectra of the grafted fabrics (Fig. 1 and Fig. S1, SM) showed the effective incorporation of the polymers. It must be stressed that in the IR spectra of the grafted samples (Fig. S1, SM), the silk fibroin bands were detected together with those assignable to the polymer, suggesting that the polymer is present on the surface of the fibres and its thickness is lower than the thickness analyzable by ATR/IR spectroscopy (i.e. 2 μm, see Experimental Section).

As previously reported [26], polymeric and silk fibroin components interact each other and are not phase separated and bonds stronger than a simple physical interaction should be present [12]. According to the literature, the residues potentially involved in these covalent interactions could be serine (through its OH group) [43-45] and glycine (through its NH group) [46].

The Raman I_{602}/I_{644} and I_{1300}/I_{644} intensity ratios proved suitable to gain relative quantitative information on the HEMA and HBA incorporation, respectively, since their trend well correlated with the % weight gain due to these components in HEMA-grafted and HBA-grafted samples (Fig. S4 (A) and (B), SM); the tyrosine band at 644 cm^{-1} [47] was used as internal standard. These ratios allowed to calculate the % weight gains ascribable to the single polymeric components in the HEMA30_HBA5-grafted and HEMA25_HBA10-grafted fabrics; the data reported in Fig. 1 (B) suggest that only a small fraction of the added HBA efficiently grafted to the fabric. This is not unexpected since methacrylic acid derivatives have been found to react with a higher efficiency than the corresponding acrylic acid derivatives [12,15]. In this light, it is not surprising that the weight gain % of the samples under study linearly increased with the percentage owf of HEMA in the grafting mixture (Fig. S9, SM), strengthening the idea that this component was the main responsible for fibre weight increase.

The quantitative data reported in Fig. 2 showed that the secondary structure distribution was nearly the same in control silk, HEMA35-grafted, HEMA30_HBA5-grafted and HEMA25_HBA10-grafted fabrics; under the used experimental conditions, the β-sheet conformation, on which the mechanical properties of silk fibroin depend [28], was kept upon grafting.

On the other hand, the Raman spectra of HEMA-grafted and HBA-grafted samples (Fig. 3 (A)) with nearly the same weight gain (26% and 25%, respectively), as well as the quantitative secondary structure data obtained through Amide I band fitting (Fig. 3 (B)), showed that the grafting with HBA had a higher impact on silk fibroin conformation than the grafting with HEMA. In fact, upon the former treatment, significant increases in the contents of β-turns occurred at the expenses of the β-sheet structure, whose amount decreased. This trend, which was not observed for the HEMA-grafted fabric, may be explained by considering the higher steric hindrance of HBA. Evidently, the higher length of the aliphatic side-chain hinders the crystallization into β-sheet conformation. This effect, which was observed since HBA weight gains of 9.7% (Fig. S5, SM), was not detected in the HEMA30_HBA5-grafted and HEMA25_HBA10-grafted fabrics, whose HBA contents were significantly lower (Fig. 1 (B)).

Vibrational spectroscopy showed that the nanofibres were conformationally more heterogeneous than the corresponding fabrics from which they were obtained. In fact, as shown in Fig. 2 (A), the full-width at half maximum (FWHM) of the Raman Amide I band increased in all the samples upon electrospinning and subsequent immersion in aqueous methanol, suggesting that the distribution of the different elements of secondary structure became wider upon these treatments. The quantitative data reported in Fig. 2 (B) showed that upon these treatments all the samples underwent significant decreases in β-sheet contents and significant increases in β-turns and unordered conformations. It is interesting to note that the changes were lower for control silk than for the other samples. This trend indicates that the

grafted polyHEMA component hindered the crystallization into β-sheet upon aqueous methanol treatment; the presence of the HBA component in the grafting mixture did not further decrease the ability of silk fibroin to rearrange into β-sheet upon the same treatments, due to its low contents under the used experimental conditions.

The SEM images of the control silk fabric show a smooth surface, whereas the grafted silk fabrics show the occurrence of fibrillation, due to the grafting treatment (Fig. 5). *B. mori* silk has a core-shell structure, consisting of two components: fibroin and sericin proteins [48]. Sericin can be easily removed by heating [49]. Once without the protection of the sericin proteins, silk fibroin is exposed outside, and the fibril and even the microfibril inside the fibroin filament can be easily split during the fabrication process. Hence, during the grafting procedure, the fibrils of silk fibroin were easily split and pulled out to the fibre surface. Fibrillation could further accumulate on the fabrics surface forming a layer of 'fuzz', so-called white stripe [50].

The membranes obtained by electrospinning were free of defects and homogenous in morphology; after aqueous methanol treatment, they maintained their fibrous structure and the average fibre diameters slightly increased (Fig. S7, SM). The pore dimension distribution (Fig. S8, SM) did not change after the aqueous methanol treatment: in all the samples most pores had sizes in the 0–0.5 μm and 0.5–1 μm ranges. This result suggests that cells cannot penetrate into the nanofibrous substrates, in the first phases of cell proliferation, at least.

Contact angle measurements showed that the nanofibres had a higher hydrophilicity than the fabrics (Fig. 6). Evidently, electrospinning and following immersion in aqueous methanol induced structural rearrangements that exposed hydrophilic groups to the fibre surface.

HEMA grafting determined a decrease in the contact angle both in the fabrics and nanofibres; this result is not surprising, since polyHEMA possesses chemical functional groups (i.e. OH groups) which are expected to increase hydrophilicity. Analogous trends have been reported in the literature for HEMA-grafted silk fibroin films [25]. The decrease in the contact angle

values indicated that the HEMA-grafting results in the exposure of hydrophilic groups towards the fibre surface; these groups belong to polyHEMA and possibly also to the silk fibroin polypeptide chain, which was found to rearrange upon grafting. It cannot be excluded that these rearrangements expose hydrophilic residues to the fibre surface. Actually, the decrease in the contact angle observed going from the control silk fabric to the corresponding nanofibrous scaffold may be explained accordingly and is in agreement with the already reported trend of the Raman I_{850}/I_{830} tyrosine ratio, which revealed an increased exposure of this hydrophilic residue [26]. Unfortunately, no information on the tyrosine environment can be obtained for the grafted samples, due to the contribution of the polymeric component to this spectral range.

Upon adding HBA in the grafting mixture, the contact angle was found to slightly increase with respect to the HEMA35-grafted samples. This trend may be explained according to the compositions of the samples as determined by Raman spectroscopy (data reported in Fig. 1 (B)), by considering that in HEMA30_HBA5-grafted and HEMA25_HBA10-grafted samples, the HEMA content was lower than in the HEMA35-grafted samples and, at the same time, the HBA content increased. HBA monomer brings an OH group as in the case of HEMA, but in the former the aliphatic chain bringing this group is longer and thus has more hydrophobic properties. It is interesting to note that the contact angle value well correlated with the % HEMA weight gain; as shown in Fig. 6 (B), at decreasing HEMA content, increases in contact angle (and thus in hydrophobicity) occurred.

Cytotoxicity tests allow the analysis of the *in vitro* viability of the cells in contact with the substrates. They are generally employed as preliminary tests to screen the ability of different substrates to affect cell behavior, as they are simple and have a high sensitivity. On the other hand, the ISO 10993-5 *in vitro* cytotoxicity test guideline [51] does not define one single standard test method but it describes testing schemes. The selection of the type of cytotoxicity test depends on the specific samples under analysis. Cytotoxicity tests are often performed for

24-72 h when screening different substrates as in our case, to give evidence of the biocompatibility of the materials in direct contact with cells.

Cell culture studies showed that after 3 days, the nanofibrous membranes behaved better than the corresponding fabrics at the same culture time (Fig. 7). These trends are not surprising since it is well known that the material surface chemistry and topography have a great influence on cell adhesion and growth [52]. Pure silk fibroin substrates have been reported to promote the growth of anchorage dependent mammalian cells, thanks to its hydrophilic nature, as well as to its ability to interact with the negative charged surface of cell membrane [1,53]. In general, moderately hydrophilic surfaces display a better affinity for cells than hydrophobic ones and improvements in cell adhesion have been reported by grafting silk fibroin with polyHEMA and even more with poly(acrylic acid) [25]; however, this parameter is not the only one determining cell adhesion since very hydrophilic silk fibroin derivatives may negatively affect cell binding [25], and the chemical nature of the groups exposed to the surface of the substrate plays a crucial role as well as topography. On the other hand, crystallinity has been reported to influence both hydrophilicity and surface roughness [54-56]. In fact, variations in crystallinity lead to changes in surface roughness on the nanometer length scale, to which cells are extremely sensitive [54,55]. Moreover, an increase in the surface crystallinity as a result of conformational changes in the amorphous domains into β-sheet has been hypothesized to contribute to an increase in surface hydrophobicity [56].

All these aspects must be taken into account to explain the data reported in Fig. 7. It is interesting to note that the conformational changes occurred in silk fabrics upon grafting with HEMA and HBA, as well as after electrospinning and treatment with aqueous methanol, did not prevent the natural cell recognition sites of the protein from being exposed towards the surface of the substrates; evidently, the surface chemistry and topography of the nanofibres appeared more favorable than those of the fabrics.

In the future, we will perform *in vitro* cell experiments on nanofibrous samples for longer

times in the perspective to screen suitable compositions for soft tissue regenerative medicine.

5. CONCLUSIONS

In this study, *B. mori* silk fabrics were successfully modified by grafting with HEMA and a binary mixture of HEMA and HBA. These substrates, as well as the corresponding nanofibrous scaffolds obtained by electrospinning from TFA and treatment with aqueous methanol, were characterized by different analytical techniques to gain information on their morphological, chemical, physical and biocompatibility properties. Vibrational spectroscopy was successfully used to gain information on the conformational rearrangements occurred in silk fibroin upon grafting as well as on the composition of the samples, on which the trend of the contact angle data were found to depend. PolyHEMA was found to hinder crystallization into β-sheet only upon electrospinning and treatment with aqueous methanol; the presence of the HBA component in the grafting mixture did not further decrease the ability of silk fibroin to rearrange into β-sheet upon the same treatments, due to its low contents (below 5%) under the used experimental conditions. However, at higher weight gains, the HBA component was found to have a higher impact on silk fibroin conformation than the grafting with HEMA.

Cell culture tests showed that the surface of the substrates under study was compatible with fibroblasts attachment and growth. The HEMA25_HBA10-grafted fabric induced a significant improvement in cell proliferation with respect to control silk fabric; the nanofibrous scaffolds under study showed a significantly higher cell growth than the fabrics, suggesting that cell adhesion and proliferation may be easily modulated by varying the surface chemistry and topography of the substrates. The results here presented demonstrate that grafting improved the surface properties of silk fibroin for enhanced functional performance in view of biomedical applications.

ACKNOWLEDGEMENTS

The authors thank Eleonora Pavoni for several vibrational spectra. This work was supported by the RFO institutional academic funds of Prof. Paola Taddei (University of Bologna).

REFERENCES

[1] C. Vepari, D.L. Kaplan, Silk as a biomaterial, Prog. Polym. Sci. 32 (2007) 991-1007.

[2] S. C. Kundu, B. Kundu, S. Talukdar, S. Bano, S. Nayak, J. Kundu, B. B. Mandal, N. Bhardwaj, M. Botlagunta, B. C. Dash, C. Acharya, A. K. Ghosh, Nonmulberry silk biopolymers, Biopolymers 97 (2012) 455-467.

[3] G.H. Altman, F. Diaz, C. Jakuba, T. Calabro, R.L. Horan, J. Chen, H. Lu, J. Richmond, D.L. Kaplan, Silk-based biomaterials, Biomaterials 24 (2003) 401-416.

[4] J. Melke, S. Midha, S. Ghosh, K. Ito, S. Hofmann, Silk fibroin as biomaterial for bone tissue engineering, Acta Biomater. 31 (2016) 1-16.

[5] S. Kapoor, S.C. Kundu, Silk protein-based hydrogels: Promising advanced materials for biomedical applications, Acta Biomater. 31 (2016) 17-32.

[6] A.E. Thurber, F.G. Omenetto, D.L. Kaplan, In vivo bioresponses to silk proteins Biomaterials 71 (2015) 145-157.

[7] B. Kundu, R. Rajkhowa, S.C. Kundu, X. Wang, Silk fibroin biomaterials for tissue regenerations, Adv. Drug Deliv. Rev. 65 (2013) 457-470.

[8] S. Sukigara, M. Gandhi, J. Ayutsede, J. Micklus, F. Ko, Regeneration of *Bombyx mori* silk by electrospinning. Part 1: processing parameters and geometric properties, Polymer 44 (2003) 5721-5727.

[9] S. Sukigara, M. Gandhi, J. Ayutsede, J. Micklus, F. Ko, Regeneration of *Bombyx mori* silk by electrospinning. Part 2. Process optimization and empirical modeling using response surface methodology, Polymer 45 (2004) 3701-3708.

[10] P. Taddei, S. Tozzi, G. Zuccheri, S. Martinotti, E. Ranzato, V. Chiono, I. Carmagnola, M. Tsukada, Intermolecular interactions between *B. mori* silk fibroin and poly(L-

lactic acid) in electrospun composite nanofibrous scaffolds, Mater. Sci. Eng. C 70 (2017) 777-787.

[11] G. Freddi, M. Tsukada, Silk fibers (grafting), in: J.C. Salamone (Ed.), Polymeric Materials Encyclopedia, vol. 10, CRC Press Inc., New York, 1996, p. 7734.

[12] G. Freddi, F.R. Massafra, S. Beretta, S. Shibata, Y. Gotoh, H. Yasui, M. Tsukada, Structure and properties of *Bombyx mori* silk fibers graft with methacrylamide (MAA) and 2-hydroxyethyl methacrylate (HEMA), J. Appl. Polym. Sci. 60 (1996) 1867-1876.

[13] M. Tsukada, G. Freddi, Y. Ishiguro, H. Shiozaki, Structural analysis of methacrylamide-grafted silk fibers, J. Appl. Polym. Sci. 50 (1993) 1519-1527.

[14] M. Tsukada, Y. Gotoh, G. Freddi, T. Yamamoto, N. Nakabayashi, Molecular weight distribution of the methyl methacrylate (MMA) polymer separated from the MMA-grafted silk fiber, J. Appl. Polym. Sci. 44 (1992) 2197-2202.

[15] M. Tsukada, G. Freddi, H. Shiozaki, N. Kasai, M. Kobayashi, Structural analysis of Poly(4-HBA)-grafted silk fibers, Angew. Makromol. Chem. 241 (1996) 19-26.

[16] M. Tsukada, G. Freddi, P. Monti, A. Bertoluzza, H. Shiozaki, Physical properties of 2-hydroxyethyl methacrylate-grafted silk fibers, J. Polym. Sci. 49 (1993) 1835-1844.

[17] X. Lou, S. Munro, S. Wang, Drug release characteristics of phase separation pHEMA sponge materials, Biomaterials 25 (2004) 5071-5080.

[18] F. Rosso, A. Barbarisi, M. Barbarisi, O. Petillo, S. Margarucci, A. Calarco, G. Peluso, New polyelectrolyte hydrogels for biomedical applications, Mater. Sci. Eng. C 23 (2003) 371-376.

[19] G.H. Hsiue, J.A. Guu, C.C. Cheng, Poly(2-hydroxyethyl methacrylate) film as a drug delivery system for pilocarpine, Biomaterials 22 (2001) 1763-1769.

[20] O. Wichterle, D. Lim, Hydrophilic Gels for Biological Use, Nature 185 (1960) 117-118.

[21] D. Klee, H. Höcker, Polymers for Biomedical Applications: Improvement of the Interface Compatibility Advances in Polymer Science, Vol. 149, Springer-Verlag,

Berlin 2000, p. 1-58.

[22] G. Lorenz, D. Klee, H. Höcker, C. Mittermayer, Characterization of surface-modified polyurethane blends, poly(vinyl alcohol), and poly(4-hydroxybutyl acrylate) for biomedical application by electron spin resonance spectroscopy, J. Appl. Polym. Sci. 57 (1995) 391-400.

[23] X. Liu, P.X. Ma, The nanofibrous architecture of poly(l-lactic acid)-based functional copolymers, Biomaterials 31 (2010) 259-269.

[24] X. Zhan, Z. Mao, J. Chen, Y. Zhang, Acrylate copolymer: a rate-controlling membrane in the transdermal drug delivery system, e-Polymers 15 (2015) 55-63.

[25] V. Dhyani, N. Singh, Controlling the cell adhesion property of silk films by graft polymerization, ACS Appl. Mater. Interfaces 6 (2014) 5005-5011.

[26] E. Pavoni, M. Tsukada, P. Taddei, Influence of grafting with acrylate compounds on the conformational rearrangements of silk fibroin upon electrospinning and treatment with aqueous methanol, J. Raman Spectrosc. 47 (2016) 1367-1374.

[27] S.H. Kim, Y.S. Nam, T.S. Lee, W.H. Park, Silk fibroin nanofiber. Electrospinning, properties, and structure, Polym. J. 35 (2003) 185-190.

[28] M. Tsukada, Y. Gotoh, M. Nagura, N. Minoura, N. Kasai, G. Freddi, Structural changes of silk fibroin membranes induced by immersion in methanol aqueous solutions, J. Polym. Sci. Part B: Polym. Phys. 32 (1994) 961-968.

[29] T. Lefèvre, M.E. Rousseau, M. Pèzolet, Protein secondary structure and orientation in silk as revealed by Raman spectromicroscopy, Biophys. J. 92 (2007) 2885–2895.

[30] F. Braut-Boucher, J. Pichon, P. Rat, M. Adolphe, M. Aubery, J. Font, A non-isotopic, highly sensitive, fluorimetric, cell-cell adhesion microplate assay using calcein AM-labeled lymphocytes, J. Immunol. Methods 178 (1995) 41-51.

[31] P. Taddei, F. Balducci, R. Simoni, P. Monti, Raman, IR and thermal study of a new highly biocompatible phosphorylcholine-based contact lens, J. Mol. Struct. 744-747

(2005) 507-514.

[32] I. Lipschitz, The vibrational spectrum of poly(methyl methacrylate): A review, Polym. Plast. Technol. Eng. 19 (1982) 53-106.

[33] H.A. Willis, V.J.I. Zichy, P.J. Hendra, The laser-Raman and infra-red spectra of poly(methyl methacrylate), Polymer 10 (1969) 737-746.

[34] P. Monti, G. Freddi, A. Bertoluzza, N. Kasai, M. Tsukada, Raman spectroscopic studies of silk fibroin from *Bombyx mori*, J. Raman Spectrosc. 29 (1998) 297-304.

[35] H.G.M. Edwards, D.W. Farwell, Raman spectroscopic studies of silk, J. Raman Spectrosc. 26 (1995) 901-909.

[36] P. Monti, P. Taddei, G. Freddi, T. Asakura, M. Tsukada, Raman spectroscopic characterization of *Bombyx mori* silk fibroin: Raman spectrum of Silk I, J. Raman Spectrosc. 32 (2001) 103-107.

[37] B.G. Frushour, J.L. Koenig, in: R.J.H. Clark, R.E. Hester (Eds.), Advances in Infrared and Raman Spectroscopy, vol. 1, Heyden, London, 1975.

[38] J. Magoshi, Y. Magoshi, Physical properties and structure of silk. II. Dynamic mechanical and dielectric properties of silk fibroin, J. Polym. Sci. 13 (1975) 1347-1351.

[39] J. Magoshi, M. Mizuide, Y. Magoshi, K. Takahashi, M. Kubo, S. Nakamura, Physical properties and structure of silk. VI. Conformational changes in silk fibroin induced by immersion in water at 2 to 130°C, J. Polym. Sci. Part B: Polym. Phys. 17 (1979) 515-520.

[40] P. Taddei, P. Monti, Vibrational IR conformational studies of model peptides representing the semi-crystalline domains of *Bombyx mori* silk fibroin, Biopolymers 78 (2005) 249-258.

[41] M. Tsukada, G. Freddi, J.S. Crighton, Structure and compatibility of poly(vinyl alcohol)-silk fibroin (PVA/SA) blend films, J. Polym. Sci. Part B: Polym. Phys. 32 (1994) 243-248.

[42] P. Taddei, M. Tsukada, G. Freddi, Affinity of protein fibres towards sulfation, J. Raman Spectrosc. 44 (2013) 190-197.

[43] M.D. Teli, D.R. Gupta, S.P. Valia, Continuous grafting of acrylic acid on mulberry silk for multifunctional effect, Int. Res. J. Eng. Technol. 2 (2015) 287-294.

[44] P. Taddei, E. Pavoni, M. Tsukada, Stability towards alkaline hydrolysis of *B. mori* silk fibroin grafted with methacrylamide, J. Raman Spectrosc. 47 (2016) 731-739.

[45] E. Pavoni, S. Tozzi, M. Tsukada, P. Taddei, Structural study on methacrylamide-grafted Tussah silk fibroin fibres, Int. J. Biol. Macromol. 88 (2016) 196-205.

[46] R.K. Das, D. Basu, A.K. Khan, A. Banerjee, Graft copolymerisation of methylmethacrylate onto silk fibre using $Ce^{+3}/K_2S_2O_8$ as redox initiator under visible light in a limited aqueous medium, Indian J. Fibre Text. Res. 23 (1998) 285-288.

[47] Tu AT. Raman Spectroscopy in Biology: Principles and Applications. John Wiley & Sons: Chichester, 1982.

[48] J.G. Hardy, L.M. Romer, T.R. Scheibel, Polymeric materials based on silk proteins, Polymer 49 (2008) 4309-4327.

[49] G.H. Altman, R.L. Horan, H.H. Lu, J. Moreau, I. Martin, J.C. Richmond, D.L. Kaplan, Silk matrix for tissue engineered anterior cruciate ligaments, Biomaterials 23 (2002) 4131-4141.

[50] S. Shang, L. Zhu, W. Chen, L. Yi, D. Qi, L. Yang, Reducing Silk Fibrillation through MMA Graft Method, Fiber Polym. 10 (2009) 807-812.

[51] ISO 10993-5, Biological evaluation of medical devices - Part 5: Tests for in vitro cytotoxicity, Geneva: International Organization for Standardization (2009).

[52] B. Kasemo, Biological surface science, Surf. Sci. 500 (2002) 656-677.

[53] K. Inuvye, M. Shigemichi, N. Kewe, M. Tsukada, Use of *Bombyx mori* silk fibroin as a substratum for cultivation of animal cells, J. Biochem. Bioph. Met. 37 (1998) 159-164.

[54] N.R. Washburn, K.M. Yamada, C.G. Simon, S.B. Kennedy, E.J. Amis, High-

throughput investigation of osteoblast response to polymer crystallinity: influence of nanometer-scale roughness on proliferation, Biomaterials 25 (2004) 1215-1224.

[55] L.R. Almeida, A.R. Martins, E.M. Fernandes, M.B. Oliveira, V.M. Correlo, I. Pashkuleva, A.P. Marques, A.S. Ribeiro, N.F. Durães, C.J. Silva, G. Bonifácio, R.A. Sousa, A.L. Oliveira, R.L. Reis, New biotextiles for tissue engineering: Development, characterization and in vitro cellular viability, Acta Biomater. 9 (2013) 8167-8181.

[56] V.P. Ribeiro, L.R. Almeida, A.R. Martins, I. Pashkuleva, A.P. Marques, A.S. Ribeiro, C.J. Silva, G. Bonifácio, R.A. Sousa, R.L. Reis, A.L. Oliveira, Influence of different surface modification treatments on silk biotextiles for tissue engineering applications, J. Biomed. Mater. Res. Part B: Appl. Biomater. 104B (2016) 496-507.

CAPTIONS FOR FIGURES

Figure 1. (A) Raman spectra of HEMA35-grafted, HEMA30_HBA5-grafted and HEMA25_HBA10-grafted silk fabrics (weight gains of 26%, 24% and 20%, respectively). The spectra of control silk fabric and polyHEMA [26] are reported for comparison. Some of the bands prevalently assignable to phenylalanine (F), tyrosine (Y) and tryptophan (W) are indicated. The bands assignable to polyHBA are indicated with a circle, those assignable to polyHEMA with an asterisk. The bands due to β-sheet (β) and unordered (Un.) conformations are indicated. (B) % weight gains of HEMA and HBA in the HEMA30_HBA5-grafted and HEMA25_HBA10-grafted fabrics, as determined by using the I_{602}/I_{644} and I_{1300}/I_{644} intensity ratios calculated from the Raman spectra of Fig. 1(A), by interpolation from the lines reported in Fig. S4 (A) and (B), SM.

Figure 2. (A) Full-width at half maximum (FWHM) of the Amide I band, as obtained from the Raman spectra of the silk fabrics and electrospun nanofibres after immersion in aqueous methanol. The data corresponding to silk control samples [26] are reported for comparison. (B) Percentages of secondary structure conformations as obtained by the curve fitting of the Raman Amide I range of control silk, HEMA35 and HEMA25_HBA10 samples (fabrics and electrospun nanofibres after immersion in aqueous methanol). The data corresponding to the HEMA30_HBA5 samples were not reported since they were not significantly different from those of the HEMA25_HBA10 samples, due to the still lower HBA content.

Figure 3. (A) Raman spectra in the Amide I range of the HEMA-grafted and HBA-grafted fabrics (weight gains of 26% and 25%, respectively). (B) Percentages of secondary structure conformations as obtained by the curve fitting of the Raman Amide I range of the same samples.

Figure 4. Raman (A) and IR (B) spectra of electrospun HEMA35-grafted, HEMA30_HBA5-grafted and HEMA25_HBA10-grafted nanofibres after immersion in aqueous methanol. The spectra of control silk nanofibres treated under the same conditions [26] are reported for

comparison.

The components having a contribution from aspartic acid (D) and glutamic acid (E) are indicated. The bands assignable to polyHBA are marked with a circle, those assignable to polyHEMA with an asterisk. The bands assignable to Silk I, β-sheet (β) and unordered (Un.) conformations are indicated.

Figure 5. SEM images of silk fabrics, as-electrospun nanofibres and nanofibres after immersion in aqueous methanol referred to the following materials: untreated control silk ((a), (b), (c)), HEMA35-grafted silk ((d), (e), (f)); HEMA30_HBA5-grafted silk ((g), (h), (i)); HEMA25_HBA10-grafted silk ((j), (k), (l)).

Figure 6. (A) Contact angle values of the silk fabrics and nanofibres after immersion in aqueous methanol. Data are average values and bars represent standard deviation. Asterisks indicate statistically significant differences. (B) Trend of the contact angle values as a function of the % HEMA weight gain (determined by weight measurements for HEMA35-grafted samples and by Raman spectroscopy for HEMA30_HBA5-grafted and HEMA25_HBA10-grafted samples, data reported in Fig. 1 (B)).

Figure 7. Cellular viability determined by calcein-AM assay of NIH 3T3 fibroblasts exposed for 1 and 3 days to the silk fabrics (A) and to the nanofibres treated with aqueous methanol (B). Values labeled with same letters are not statistically different from each other, whereas different letters indicate statistical differences ($P < 0.01$). The asterisks indicate significant differences between fabric and corresponding nanofibres, at each culture time.

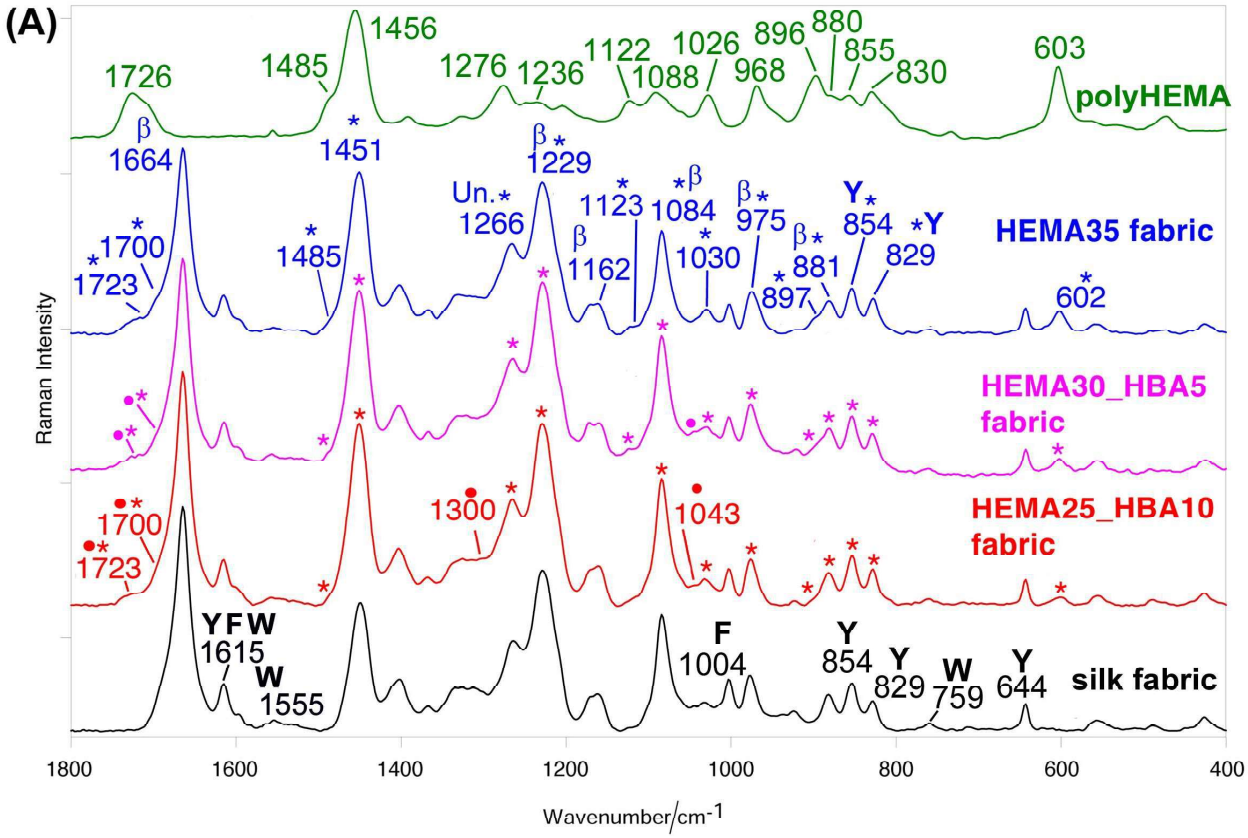
(A)
polyHEMA
HEMA35 fabric
HEMA30_HBA5 fabric
HEMA25_HBA10 fabric
silk fabric
Raman Intensity
Wavenumber/cm-1
1800
1600
1400
1200
1000
800
600
400

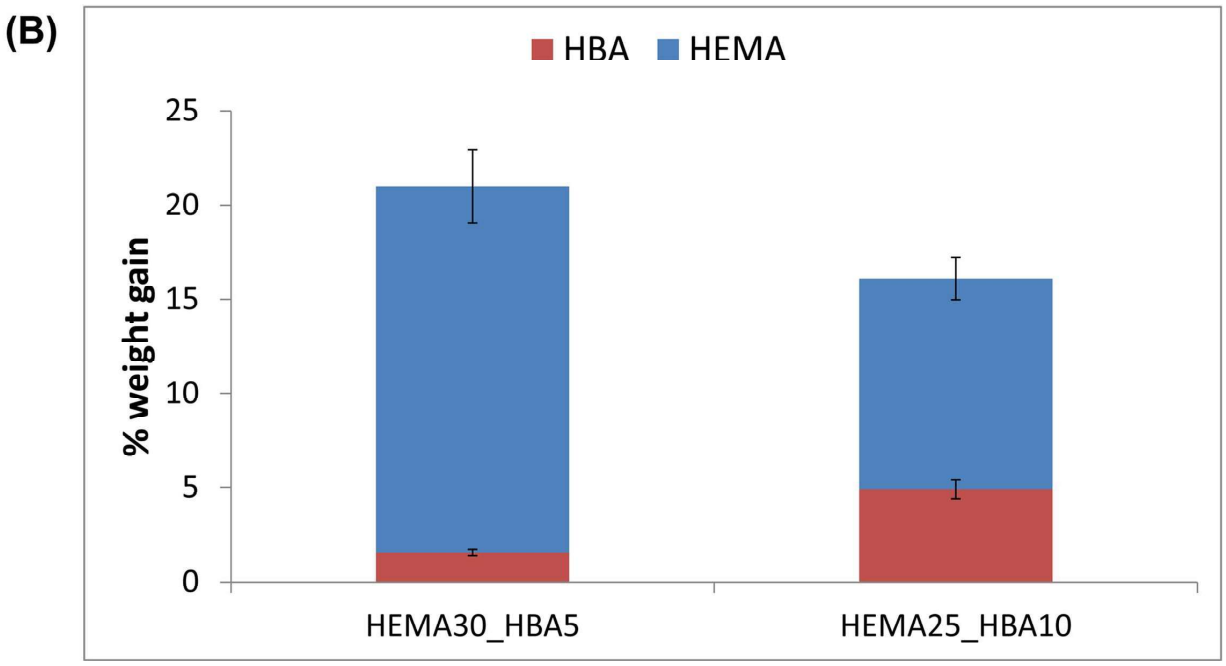
(B)
HBA
HEMA
% weight gain
25
20
15
10
5
0
HEMA30_HBA5
HEMA25_HBA10

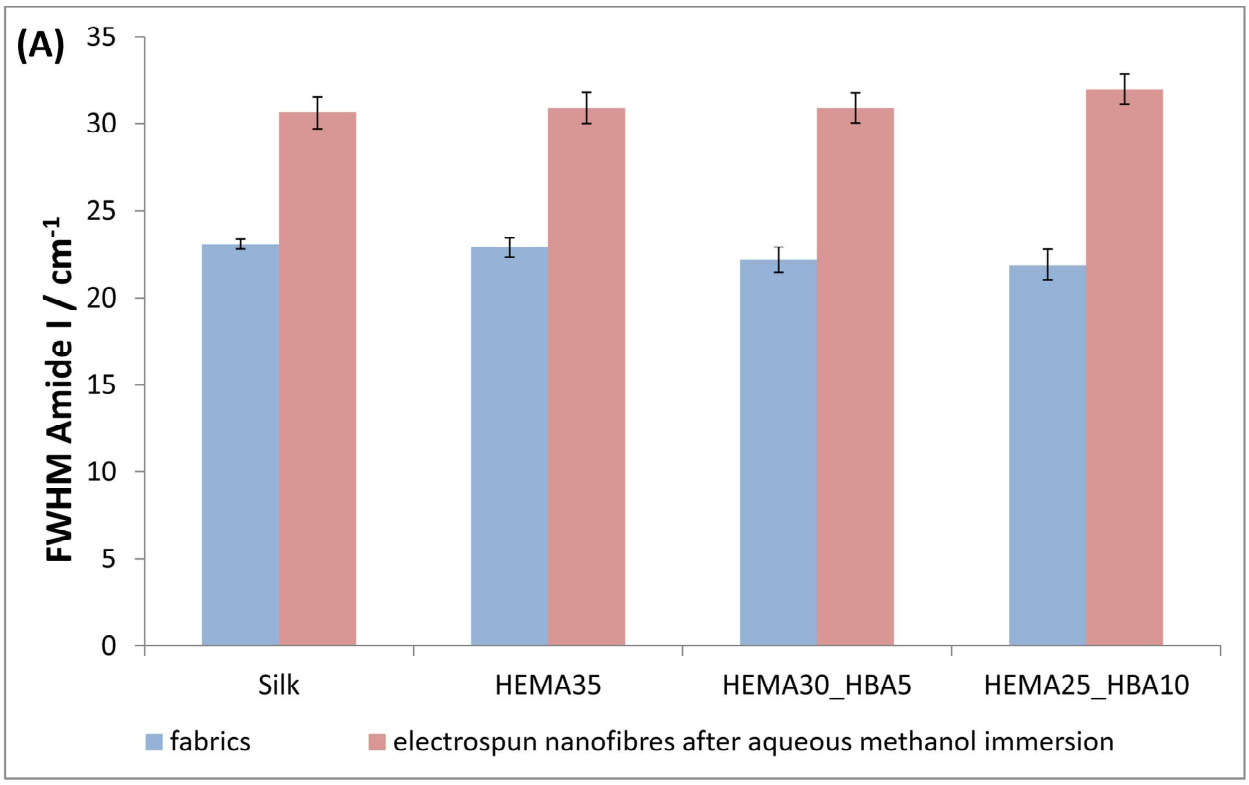
(A)
FWHM Amide I / cm-1
35
30
25
20
15
10
5
0
Silk
HEMA35
HEMA30_HBA5
HEMA25_HBA10
fabrics
electrospun nanofibres after aqueous methanol immersion

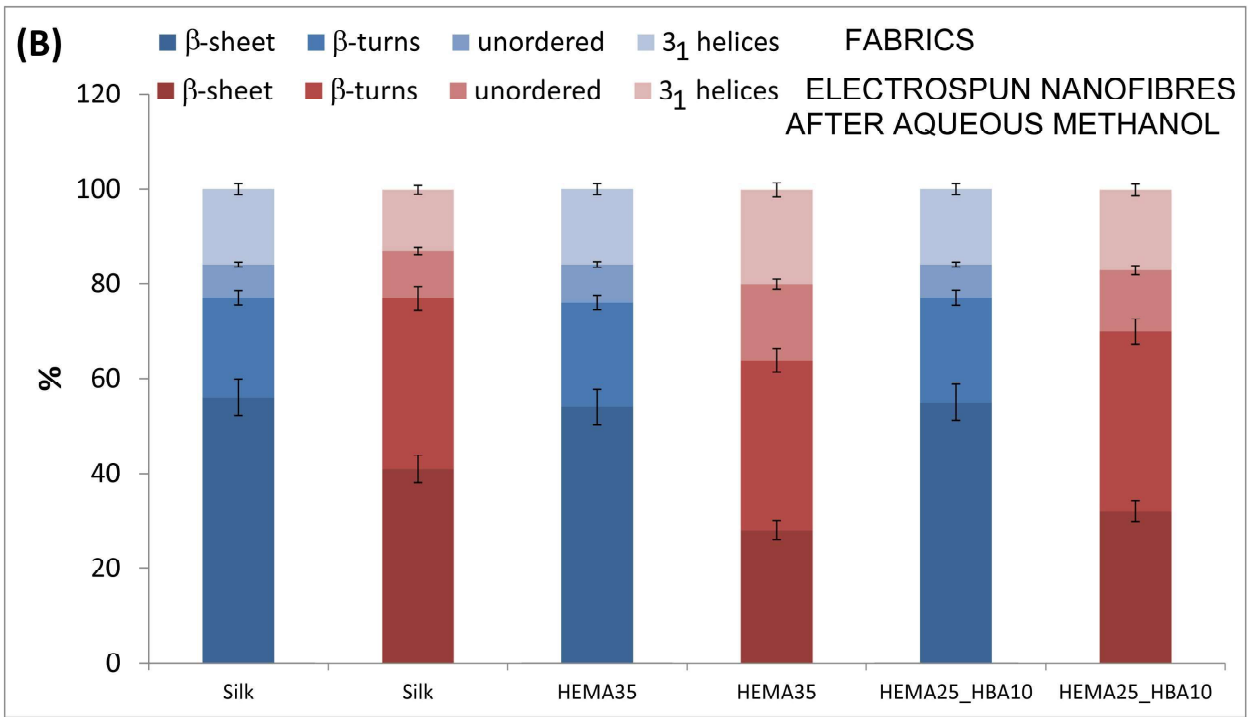
(B)
β-sheet
β-turns
unordered
31 helices
FABRICS
β-sheet
β-turns
unordered
31 helices
ELECTROSPUN NANOFIBRES AFTER AQUEOUS METHANOL
%
120
100
80
60
40
20
0
Silk
Silk
HEMA35
HEMA35
HEMA25_HBA10
HEMA25_HBA10

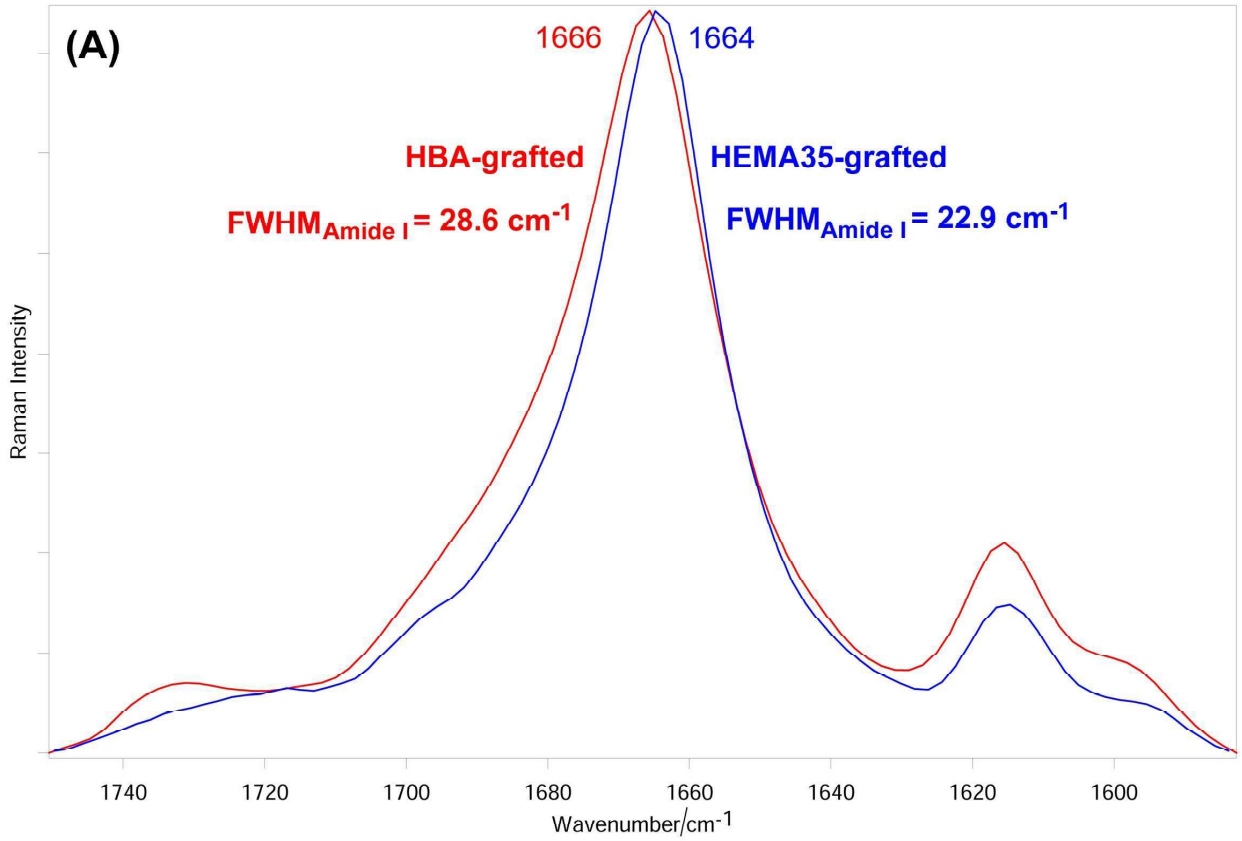
(A)
1666
1664
HBA-grafted
HEMA35-grafted
FWHMAmide I = 28.6 cm-1
FWHMAmide I = 22.9 cm-1
Raman Intensity
1740
1720
1700
1680
1660
1640
1620
1600
Wavenumber/cm-1

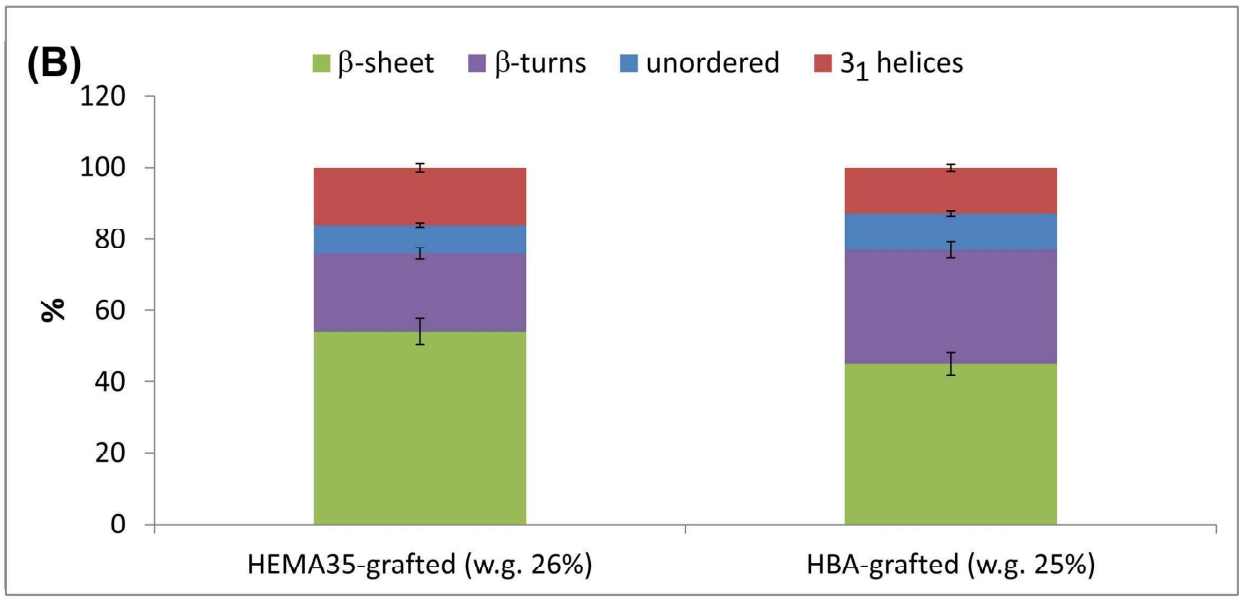
(B)
β-sheet
β-turns
unordered
31 helices
120
100
80
60
40
20
0
%
HEMA35-grafted (w.g. 26%)
HBA-grafted (w.g. 25%)

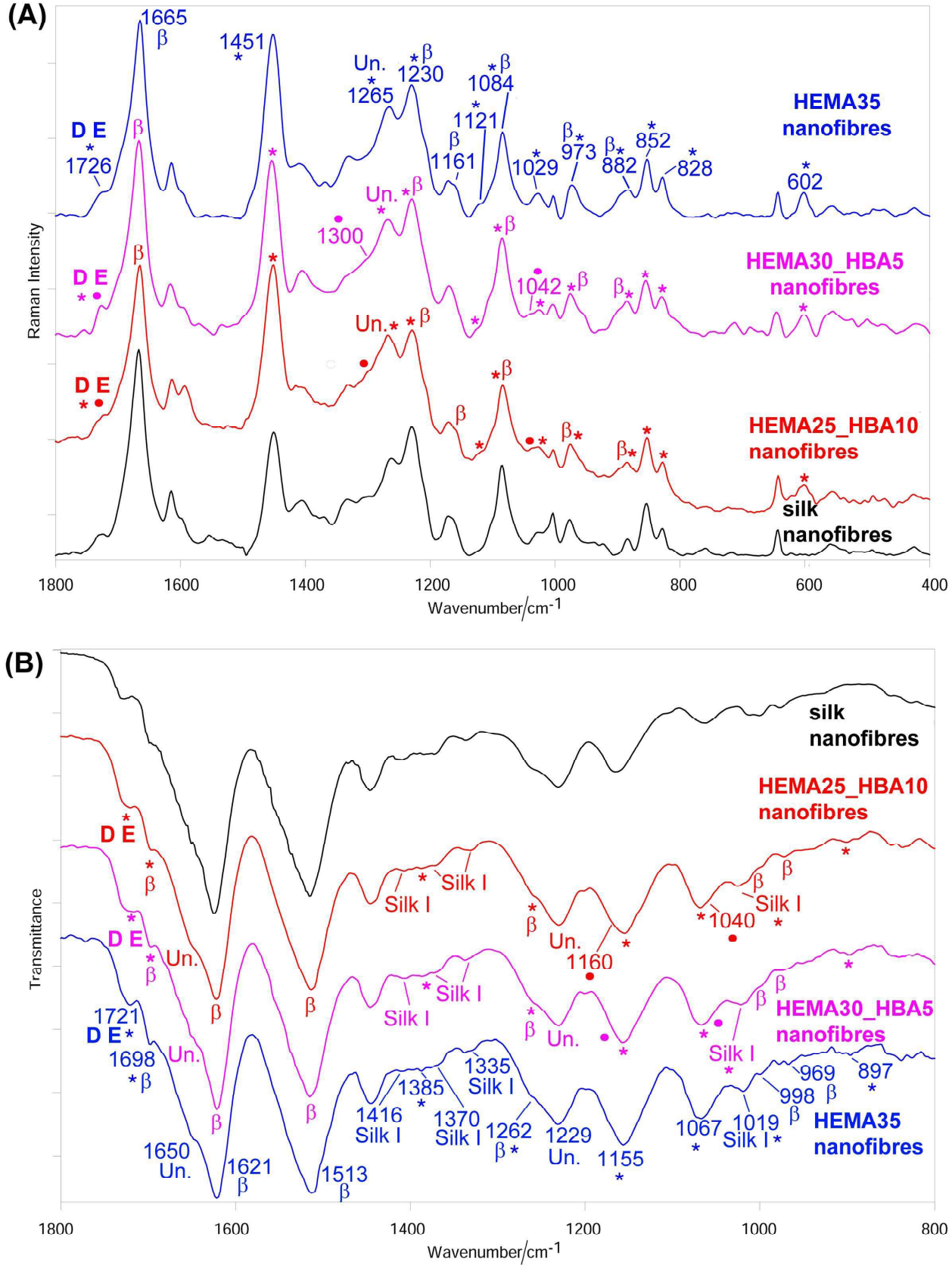
(A)
Raman Intensity
Wavenumber/cm-1
1800
1600
1400
1200
1000
800
600
400
HEMA35 nanofibres
HEMA30_HBA5 nanofibres
HEMA25_HBA10 nanofibres
silk nanofibres
1665
1451
1265
1230
1084
1121
1161
1029
973
882
852
828
602
1726
1300
1042
(B)
Transmittance
Wavenumber/cm-1
1800
1600
1400
1200
1000
800
silk nanofibres
HEMA25_HBA10 nanofibres
HEMA30_HBA5 nanofibres
HEMA35 nanofibres
Silk I
1040
1160
1721
1698
1650
1621
1513
1416
1385
1370
1335
1262
1229
1155
1067
1019
998
969
897

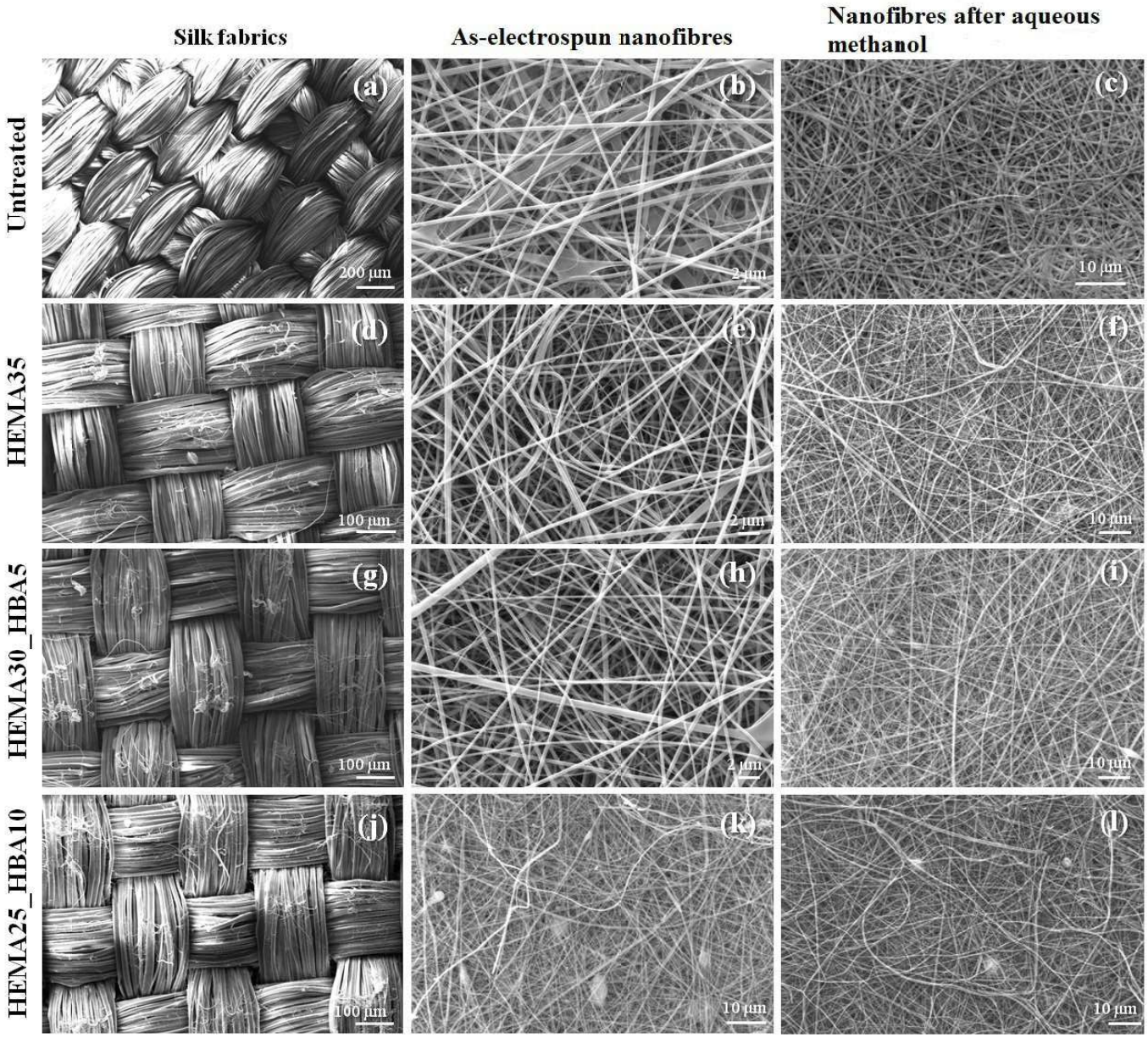
Silk fabrics
As-electrospun nanofibres
Nanofibres after aqueous methanol
Untreated
HEMA35
HEMA30_HBA5
HEMA25_HBA10
(a)
(b)
(c)
(d)
(e)
(f)
(g)
(h)
(i)
(j)
(k)
(l)
200 µm
2 µm
10 µm
100 µm
2 µm
10 µm
100 µm
2 µm
10 µm
100 µm
10 µm
10 µm

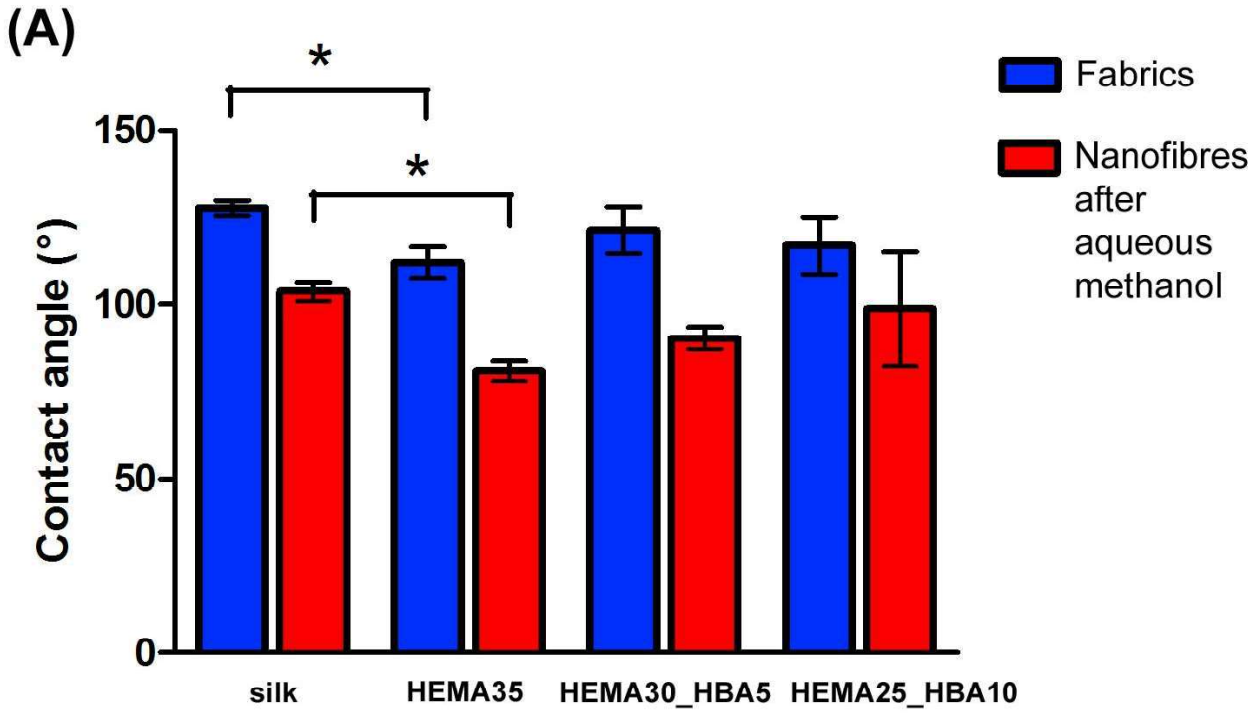
(A)
*
*
150
100
50
0
Contact angle (°)
Fabrics
Nanofibres after aqueous methanol
silk
HEMA35
HEMA30_HBA5
HEMA25_HBA10

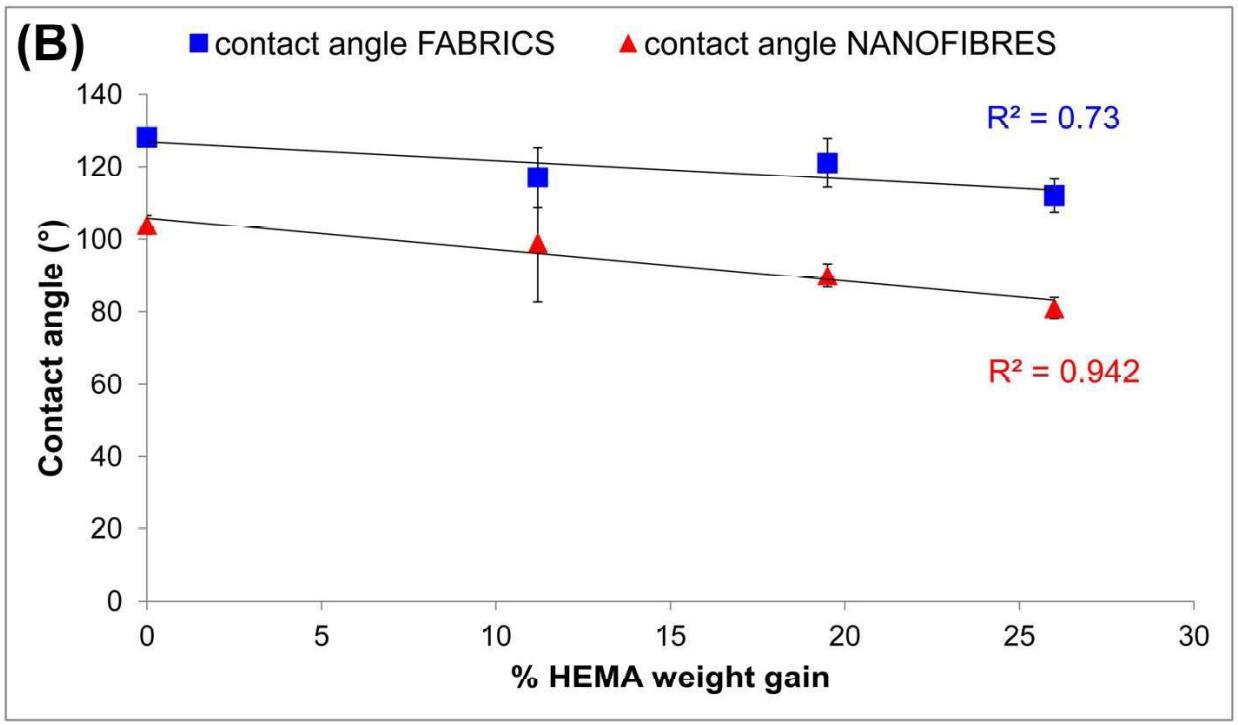
(B)
contact angle FABRICS
contact angle NANOFIBRES
R² = 0.73
R² = 0.942
140
120
100
80
60
40
20
0
Contact angle (°)
0
5
10
15
20
25
30
% HEMA weight gain

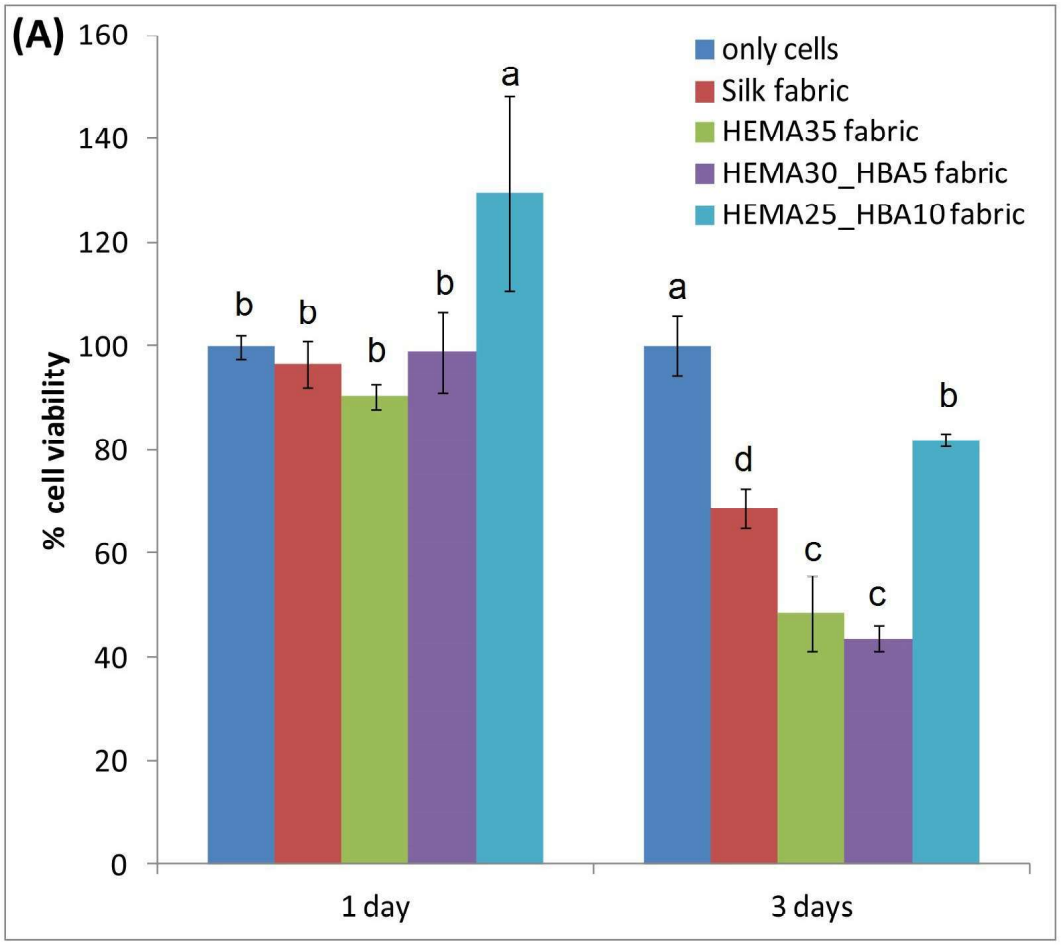
(A)
160
140
120
100
80
60
40
20
0
% cell viability
only cells
Silk fabric
HEMA35 fabric
HEMA30_HBA5 fabric
HEMA25_HBA10 fabric
b
b
b
b
a
a
d
c
c
b
1 day
3 days

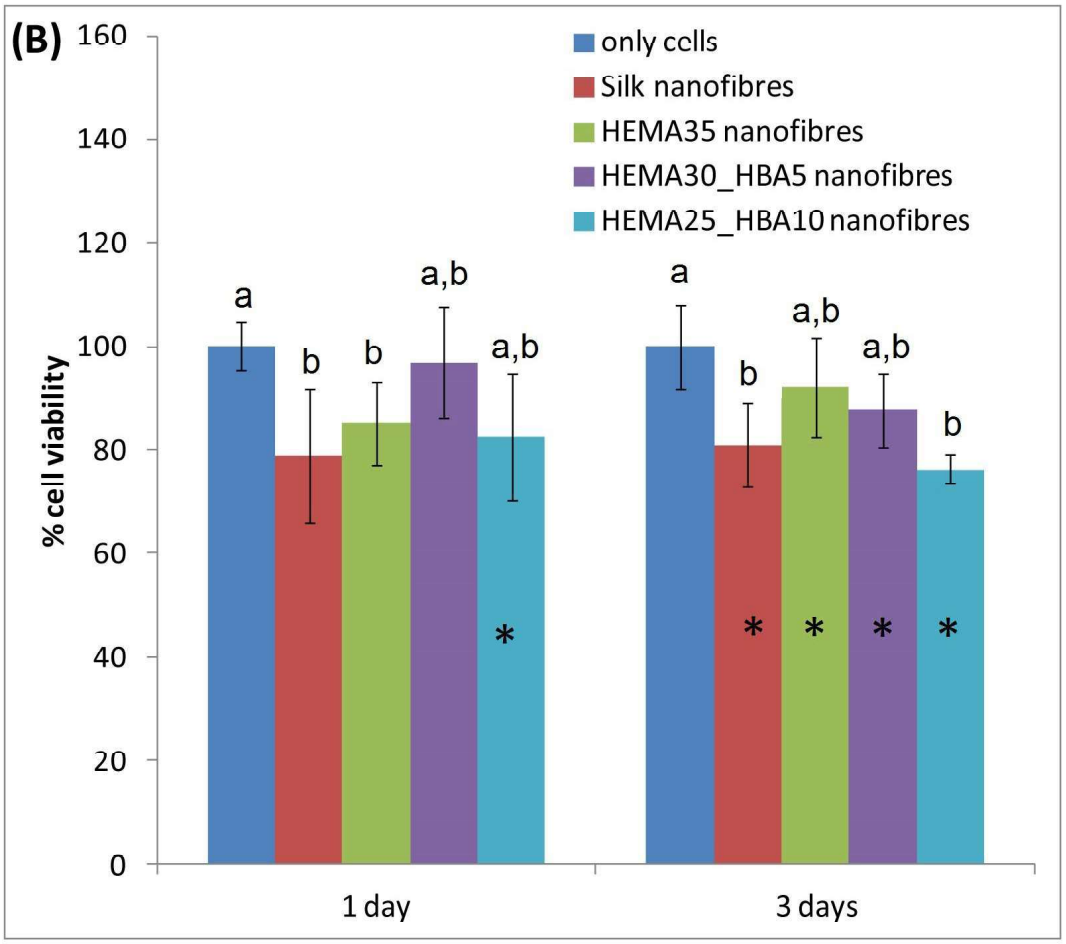
(B)
160
140
120
100
80
60
40
20
0
% cell viability
only cells
Silk nanofibres
HEMA35 nanofibres
HEMA30_HBA5 nanofibres
HEMA25_HBA10 nanofibres
a
b
b
a,b
a,b
*
a
b
a,b
a,b
b
*
*
*
*
1 day
3 days

SUPPLEMENTARY MATERIAL

SILK FIBRES GRAFTED WITH 2-HYDROXYETHYL METHACRYLATE (HEMA) AND 4-HYDROXYBUTYL ACRYLATE (HBA) FOR BIOMEDICAL APPLICATIONS

Paola Taddei,[1*] Michele Di Foggia,[1] Simona Martinotti,[2] Elia Ranzato,[3] Irene Carmagnola,[4] Valeria Chiono,[4] Masuhiro Tsukada[5]

[1] Department of Biomedical and Neuromotor Sciences, University of Bologna, Via Belmeloro 8/2, 40126 Bologna, Italy

[2] Department of Sciences and Technological Innovation, University of Eastern Piedmont, Viale Teresa Michel 11, 15121 Alessandria, Italy

[3] Department of Sciences and Technological Innovation, University of Eastern Piedmont, Piazza Sant'Eusebio 5, 13100 Vercelli, Italy

[4] Department of Mechanical and Aerospace Engineering, Politecnico di Torino, Corso Duca degli Abruzzi 24, 10129 Turin, Italy

[5] Division of Applied Biology, Faculty of Textile Science and Technology, Shinshu University, Ueda, Nagano, Japan

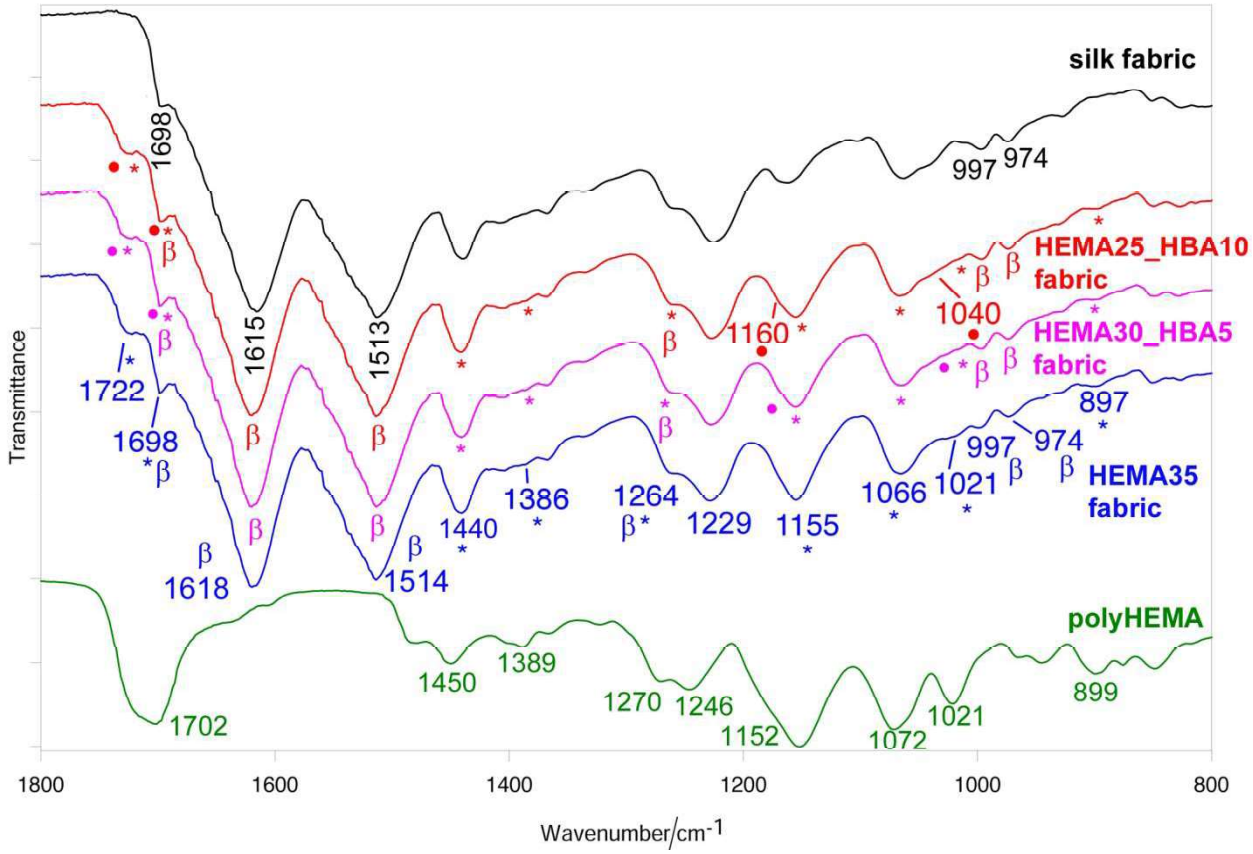

Figure S1. IR spectra of HEMA35-grafted, HEMA30_HBA5-grafted and HEMA25_HBA10-grafted silk fabrics (weight gains of 26%, 24% and 20%, respectively). The spectra of control silk fabric and polyHEMA [26] are reported for comparison. The bands assignable to polyHBA are indicated with a circle, those assignable to polyHEMA with an asterisk. The bands assignable to β-sheet (β) conformation are indicated.

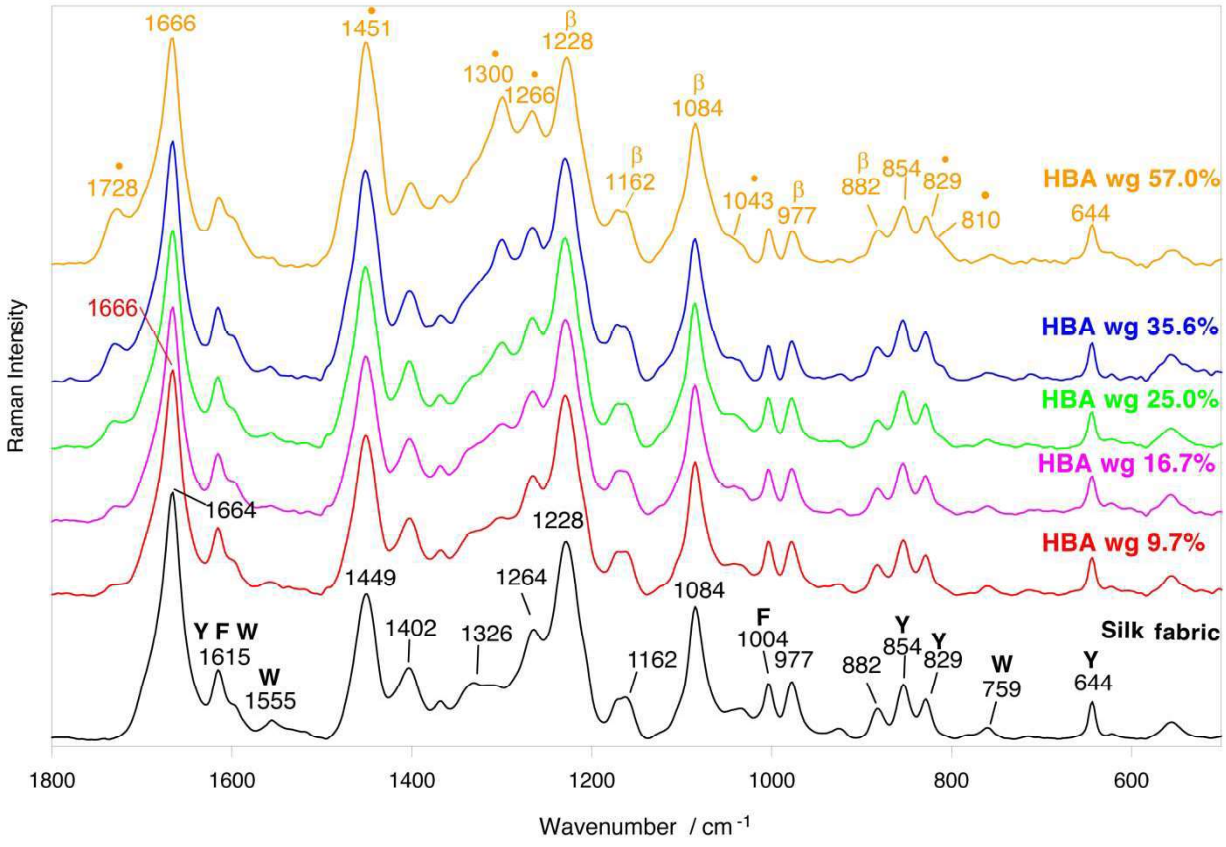

Figure S2. Raman spectra of the silk fabrics before and after grafting with HBA (weight gains of 9.7%, 16.7%, 25.0%, 35.6% and 57.0%). The spectra are normalized to the intensity of the Tyr band at 644 cm^{-1}. Some of the bands prevalently assignable to phenylalanine (F), tyrosine (Y) and tryptophan (W) are indicated. The bands assignable to polyHBA are indicated with a circle. The bands due to β-sheet (β) conformation are indicated.

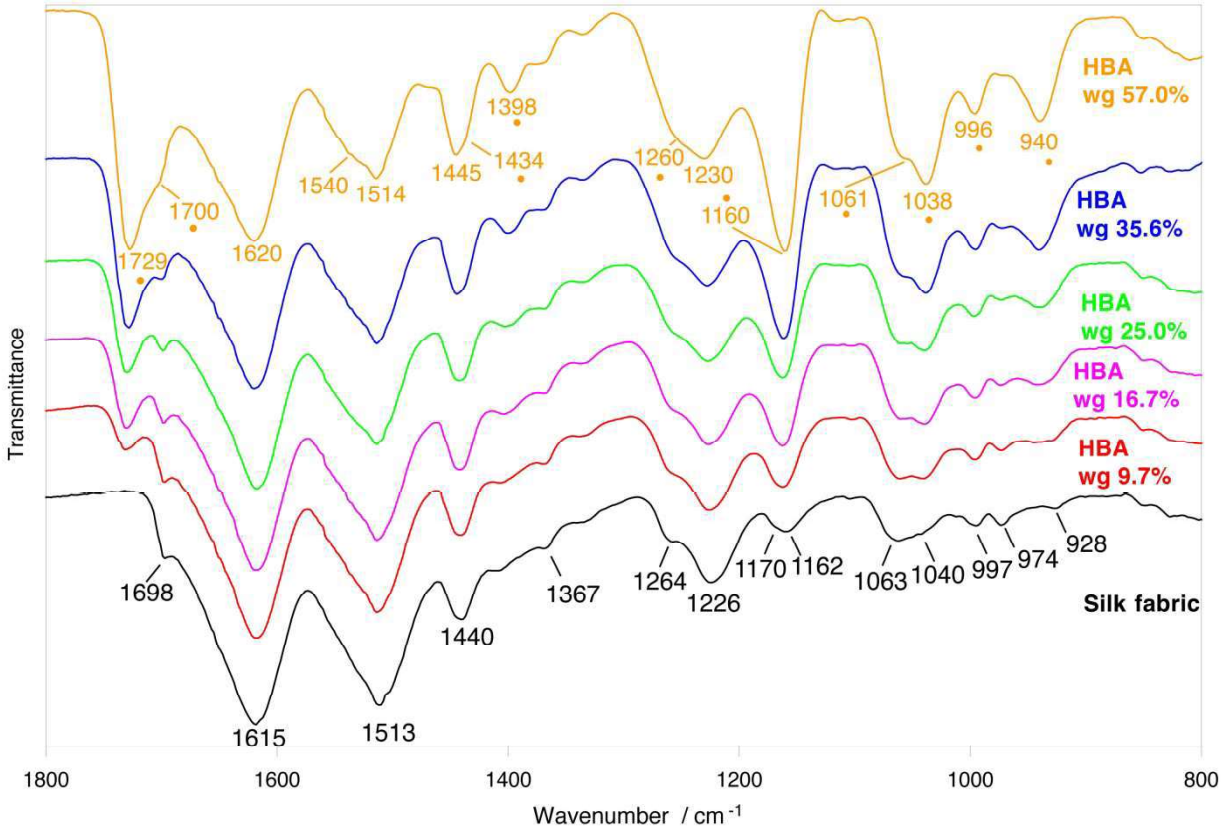

Figure S3. IR spectra of the silk fabrics before and after grafting with HBA (weight gains of 9.7%, 16.7%, 25.0%, 35.6% and 57.0%). The bands assignable to polyHBA are indicated with a circle.

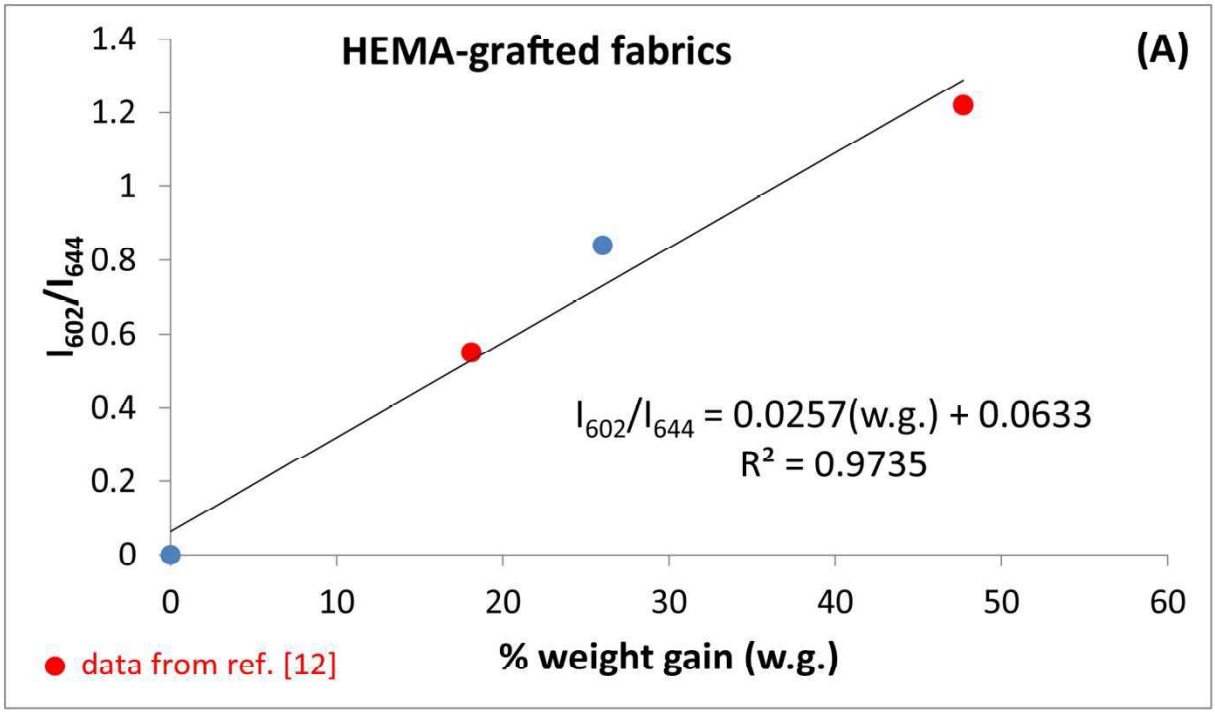

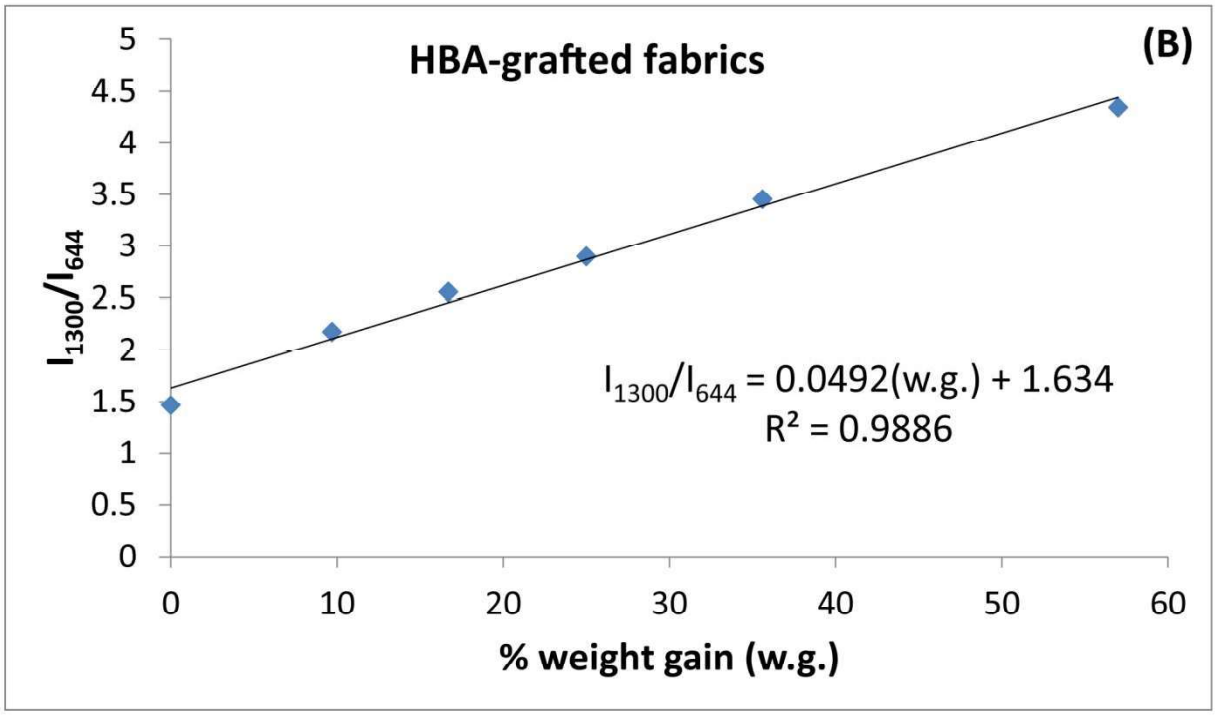

Figure S4. Trend of the Raman I_{602}/I_{644} (A) and I_{1300}/I_{644} (B) intensity ratios as a as a function of the % weight gain. The I_{602}/I_{644} values were calculated from the Raman spectrum of the HEMA35-grafted fabric (Fig. 1(A)) as well as from data reported in the literature on other HEMA-grafted samples (with weight gains of 18.1% and 47.7%) [12]. The I_{1300}/I_{644} values were calculated from the spectra reported in Fig. S2, Supplementary Material.

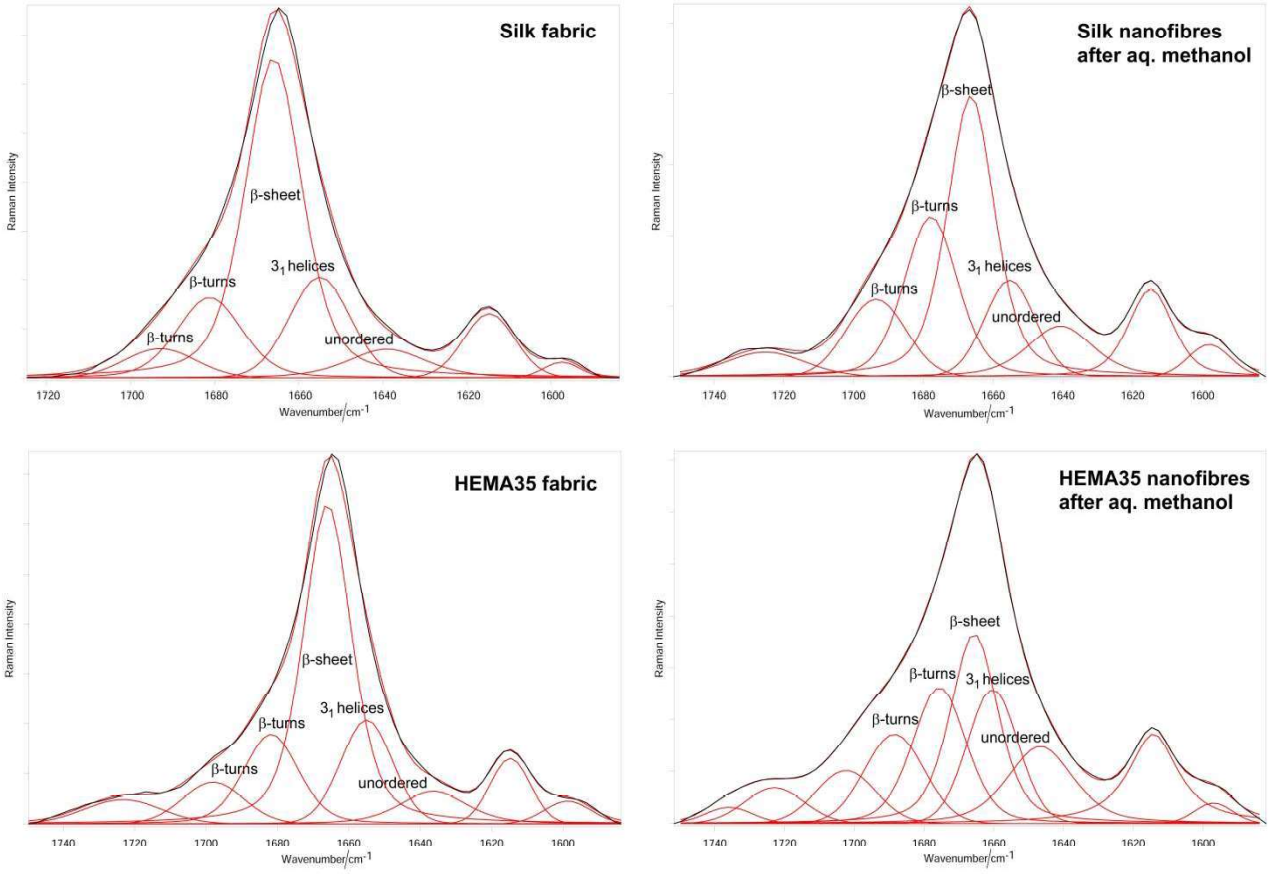

Figure S5. Experimental (black) and fitted (red) Raman Amide I region; the fitted components are shown.

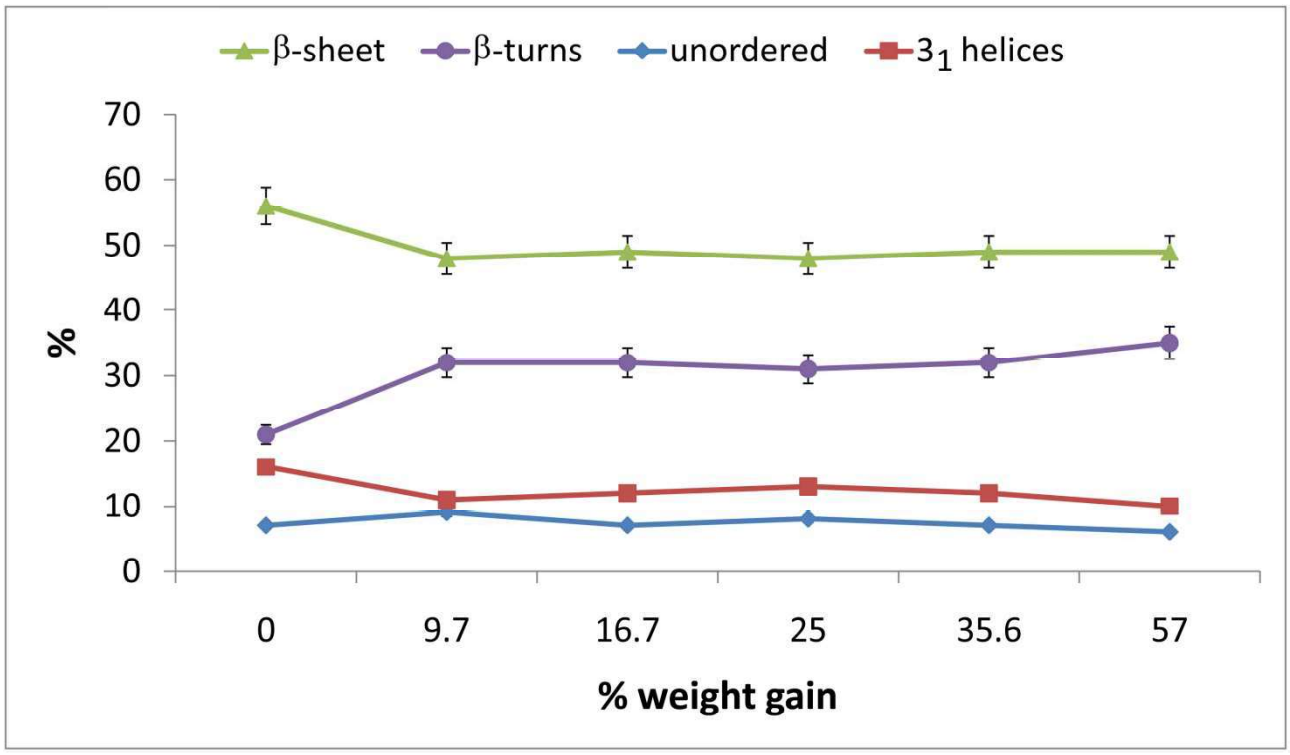

Figure S6. Trend of the secondary structures contents as a function of the % HBA weight gain, as obtained from the fitting of the Raman Amide I range of the HBA-grafted samples (Figure S2, Supplementary Material).

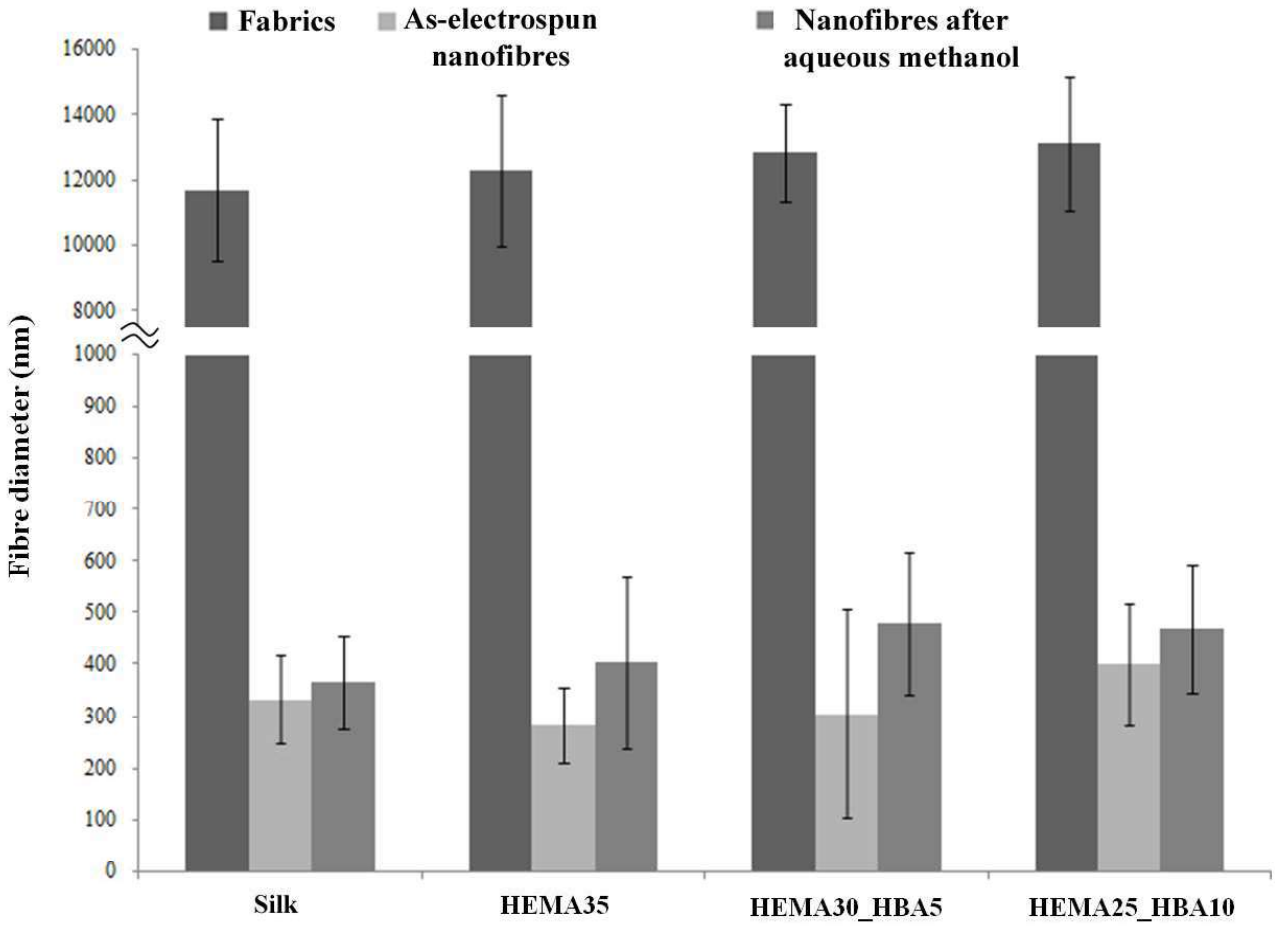

Figure S7. Fibre diameters of silk fabrics, as-electrospun nanofibres and nanofibres after immersion in aqueous methanol: control silk, HEMA35-grafted, HEMA30_HBA5-grafted and HEMA25_HBA10-grafted silk. Columns are the average values, bars represent the standard deviation.

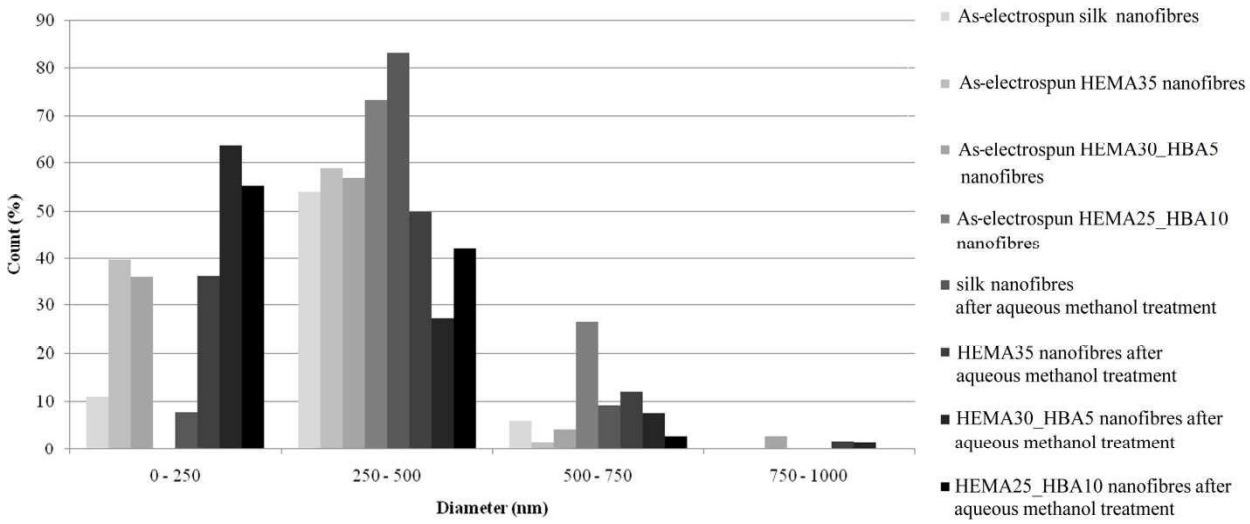

Figure S8. Pore size distribution in as-electrospun control silk, HEMA35-grafted, HEMA25_HBA10-grafted and HEMA30_HBA10-grafted nanofibres after immersion in aqueous methanol.

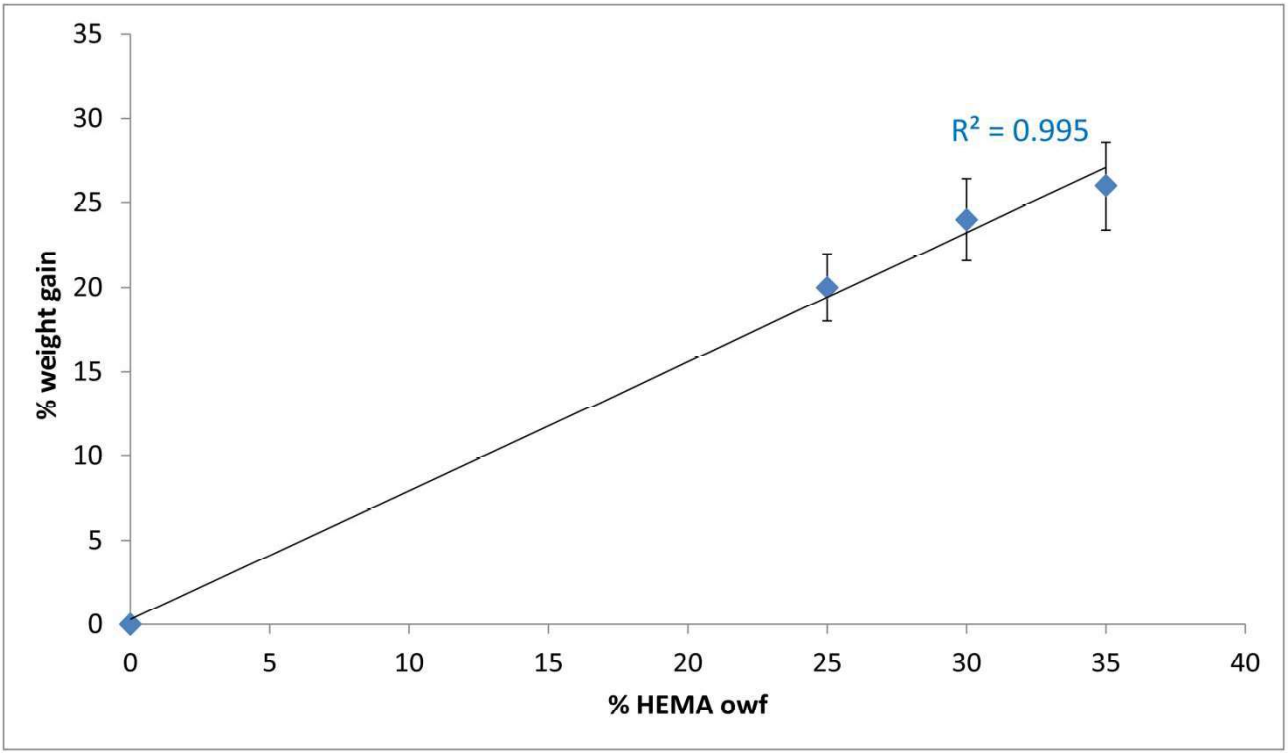

Figure S9. Trend of the % weight gain of the grafted fabrics under study as a function of the % owf of HEMA in the grafting mixture.